

Theory of Polarization: A Modern Approach

Raffaele Resta^{1,2} and David Vanderbilt³

¹ INFN–DEMOCRITOS National Simulation Center,
Via Beirut 4, I-34014, Trieste, Italy
`resta@democritos.it`

² Dipartimento di Fisica Teorica, Università di Trieste,
Strada Costiera 11, I-34014, Trieste, Italy

³ Department of Physics and Astronomy, Rutgers University,
136 Frelinghuysen Road, Piscataway, NJ 08854-8019, USA
`dhv@physics.rutgers.edu`

Abstract. In this Chapter we review the physical basis of the modern theory of polarization, emphasizing how the polarization can be defined in terms of the accumulated adiabatic flow of current occurring as a crystal is modified or deformed. We explain how the polarization is closely related to a Berry phase of the Bloch wavefunctions as the wavevector is carried across the Brillouin zone, or equivalently, to the centers of charge of Wannier functions constructed from the Bloch wavefunctions. A resulting feature of this formulation is that the polarization is formally defined only modulo a “quantum of polarization” – in other words, that the polarization may be regarded as a multi-valued quantity. We discuss the consequences of this theory for the physical understanding of ferroelectric materials, including polarization reversal, piezoelectric effects, and the appearance of polarization charges at surfaces and interfaces. In so doing, we give a few examples of realistic calculations of polarization-related quantities in perovskite ferroelectrics, illustrating how the present approach provides a robust and powerful foundation for modern computational studies of dielectric and ferroelectric materials.

1 Why is a Modern Approach Needed?

The macroscopic polarization is the most essential concept in any phenomenological description of dielectric media [1]. It is an intensive vector quantity that intuitively carries the meaning of electric dipole moment per unit volume. The presence of a spontaneous (and switchable) macroscopic polarization is the defining property of a ferroelectric (FE) material, as the name itself indicates (“*ferroelectric*” modeled after *ferromagnetic*), and the macroscopic polarization is thus central to the whole physics of FEs.

Despite its primary role in all phenomenological theories and its overwhelming importance, the macroscopic polarization has long evaded microscopic understanding, not only at the first-principles level, but even at the level of sound microscopic models. What really happens inside a FE and, more generally, inside a polarized dielectric? The standard picture is almost invariably based on the venerable Clausius–Mossotti (CM) model [2, 3], in which the presence of identifiable polarizable units is assumed. We shall show that

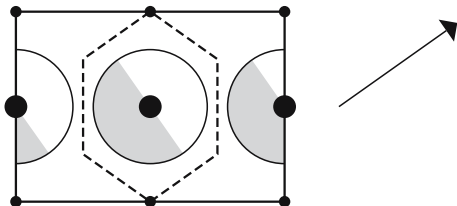


Fig. 1. A polarized ionic crystal having the NaCl structure, as represented within an extreme Clausius–Mossotti model. We qualitatively sketch the electronic polarization charge (*shaded areas indicate negative regions*) in the $(1\bar{1}0)$ plane linearly induced by a constant field \mathcal{E} in the $[111]$ direction as indicated by the arrow. The anions (*large circles*) are assumed to be polarizable, while the cations (*small circles*) are not. The boundary of a Wigner–Seitz cell, centered at the anion, is also shown (*dashed line*)

such an extreme model is neither a realistic nor a useful one, particularly for FE materials.

Experimentalists have long taken the pragmatic approach of measuring polarization *differences* as a way of accessing and extracting values of the “polarization itself”. In the early 1990s it was realized that, even at the theoretical level, polarization differences are conceptually more fundamental than the “absolute” polarization. This change of paradigm led to the development of a new theoretical understanding, involving formal quantities such as Berry phases and Wannier functions, that has come to be known as the “modern theory of polarization”. The purpose of the present chapter is to provide a pedagogical introduction to this theory, to give a brief introduction to its computational implementation, and to discuss its implications for the physical understanding of FE materials.

1.1 Fallacy of the Clausius–Mossotti Picture

Within the CM model the charge distribution of a polarized condensed system is regarded as the superposition of localized contributions, each providing an electric dipole. In a crystalline system the CM macroscopic polarization \mathbf{P}_{CM} is *defined* as the sum of the dipole moments in a given cell divided by the cell volume. We shall contrast this view with a more realistic microscopic picture of the phenomenon of macroscopic polarization.

An extreme CM view of a simple ionic crystal having the NaCl structure is sketched in Fig. 1. The essential point behind the CM view is that the distribution of the induced charge is resolved into contributions that can be ascribed to identifiable “polarization centers”. In the sketch of Fig. 1 these are the anions, while in the most general case they may be atoms, molecules, or even bonds. This partitioning of the polarization charge is obvious in Fig. 1, where the individual localized contributions are drawn as nonoverlapping.

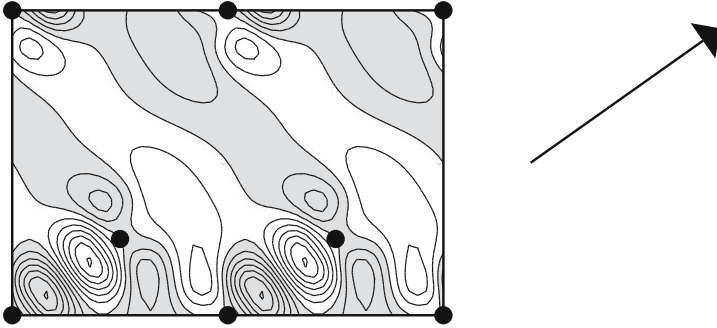


Fig. 2. Induced (pseudo)charge density $\rho^{(\text{ind})}(\mathbf{r})$ in the $(\bar{1}\bar{1}0)$ plane linearly induced by a constant field \mathcal{E} in the $[111]$ direction, indicated by the arrow, in crystalline silicon. The field has unit magnitude (in a.u.) and the contours are separated by 30 charge units per cell. Shaded areas indicate regions of negative charge; circles indicate atomic positions

But what about real materials? This is precisely the case in point: the electronic polarization charge in a crystal has a periodic continuous distribution, which cannot be unambiguously partitioned into localized contributions.

In typical FE oxides the bonding has a mixed ionic/covalent character [4], with a sizeable fraction of the electronic charge being shared among ions in a delocalized manner. This fact makes any CM picture totally inadequate. In order to emphasize this feature, we take as a paradigmatic example the extreme covalent case, namely, crystalline silicon. In this material, the valence-electron distribution essentially forms a continuous tetrahedral network, and cannot be unambiguously decomposed into either atomic or bond contributions. We show in Fig. 2 the analog of Fig. 1 for this material, with the electronic distribution polarized by an applied field along the $[111]$ direction. The calculation is performed in a first-principle framework using a pseudopotential implementation of density-functional theory [5, 6]; the quantity actually shown is the induced polarization *pseudo*charge of the valence electrons.

Clearly, the induced charge is delocalized throughout the cell and any partition into localized polarization centers, as needed for establishing a CM picture, is largely arbitrary. Looking more closely at the continuous polarization charge of Fig. 2, one notices that in the regions of the bonds parallel to the field the induced charge indeed shows a dipolar shape. It is then tempting to identify the CM polarization centers with these bond dipoles, but we shall show that such an identification would be incorrect. The clamped-ion (also called static high-frequency) dielectric tensor [7, 8] can be defined as

$$\varepsilon_{\infty} = 1 + 4\pi\chi = 1 + 4\pi \frac{\partial \mathbf{P}}{\partial \mathcal{E}}, \quad (1)$$

where \mathbf{P} is the macroscopic polarization and \mathcal{E} is the (screened) electric field. One would like to replace \mathbf{P} with \mathbf{P}_{CM} , i.e., the induced bond dipole per

cell. However, in order to actually evaluate \mathbf{P}_{CM} , one must choose a recipe for truncating the integration to a local region, which is largely arbitrary. Even more importantly, no matter which reasonable recipe one adopts, the magnitude of \mathbf{P}_{CM} is far too small (by at least an order of magnitude) to reproduce the actual value $\varepsilon_\infty \simeq 12$ in silicon. The magnitude of the local dipoles seen in Fig. 2 may therefore account for only a small fraction of the actual \mathbf{P} value for this material. In fact, as we shall explain below, it is generally *impossible* to obtain the value of \mathbf{P} from the induced charge density alone.

1.2 Fallacy of Defining Polarization via the Charge Distribution

Given that \mathbf{P} carries the meaning of electric dipole moment per unit volume, it is tempting to try to define it as the dipole of the macroscopic sample divided by its volume, i.e.,

$$\mathbf{P}_{\text{samp}} = \frac{1}{V_{\text{samp}}} \int_{\text{samp}} d\mathbf{r} \mathbf{r} \rho(\mathbf{r}). \quad (2)$$

We focus, once more, on the case of crystalline silicon polarized by an external field along the [111] direction. In order to apply (2), we need to assume a macroscopic but *finite* crystal. But the integral then has contributions from both the surface and the bulk regions, which cannot be easily disentangled. In particular, suppose that a cubic sample of dimensions $L \times L \times L$ has its surface preparation changed in such a way that a new surface charge density $\Delta\sigma$ appears on the right face and $-\Delta\sigma$ on the left; this will result in a change of dipole moment scaling as L^3 , and thus, a change in the value of \mathbf{P}_{samp} , despite the fact that the conditions in the interior have not changed. Thus, (2) is not a useful *bulk* definition of polarization; and even if it were, there would be no connection between it and the induced periodic charge density in the sample interior that is illustrated in Fig. 2.

A second tempting approach to a definition of the bulk polarization is via

$$\mathbf{P}_{\text{cell}} = \frac{1}{V_{\text{cell}}} \int_{\text{cell}} d\mathbf{r} \mathbf{r} \rho(\mathbf{r}), \quad (3)$$

where the integration is carried out over one unit cell deep in the interior of the sample. However, this approach is also flawed, because the result of (3) depends on the shape and location of the unit cell. (Indeed, the average of \mathbf{P}_{cell} over all possible translational shifts is easily shown to vanish.) It is only within an extreme CM model – where the periodic charge can be decomposed with no ambiguity by choosing, as in Fig. 1, the cell boundary to lie in an interstitial region of vanishing charge density – that \mathbf{P}_{cell} is well defined. However, in many materials a CM model is completely inappropriate, as discussed above.

As a third approach, one might imagine defining \mathbf{P} as the cell average of a microscopic polarization $\mathbf{P}_{\text{micro}}$ defined via

$$\nabla \cdot \mathbf{P}_{\text{micro}}(\mathbf{r}) = -\rho(\mathbf{r}). \quad (4)$$

However, the above equation does *not* uniquely define $\mathbf{P}_{\text{micro}}(\mathbf{r})$, since any divergence-free vector field, and in particular any constant vector, can be added to $\mathbf{P}_{\text{micro}}(\mathbf{r})$ without affecting the left-hand side of (4).

The conclusion to be drawn from the above discussion is that a knowledge of the periodic electronic charge distribution in a polarized crystalline solid cannot, even in principle, be used to construct a meaningful definition of bulk polarization. This has been understood, and similar statements have appeared in the literature, since at least 1974 [9]. However, this important message has not received the wide appreciation it deserves, nor has it reached the most popular textbooks [7, 8].

These conclusions may appear counterintuitive and disturbing, since one reasonably expects that the macroscopic polarization in the bulk region of a solid should be determined by what “happens” in the bulk. But this is precisely the basis of a third, and finally rewarding, approach to the problem, in which one focuses on the *change* in \mathbf{P}_{samp} that occurs during some process such as the turning on of an external electric field. The change in internal polarization $\Delta\mathbf{P}$ that we seek will then be given by the change $\Delta\mathbf{P}_{\text{samp}}$ of (2), *provided* that any charge that is pumped to the surface is not allowed to be conducted away. (Thus, the sides of the sample must be insulating, there must be no grounded electrodes, etc.) Actually, it is preferable simply to focus on the charge *flow* in the interior of the sample during this process, and write

$$\Delta\mathbf{P} = \int dt \frac{1}{V_{\text{cell}}} \int_{\text{cell}} d\mathbf{r} \mathbf{j}(\mathbf{r}, t). \quad (5)$$

This equation is the basis of the modern theory of polarization that will be summarized in the remainder of this chapter. Again, it should be emphasized that the definition (5) has nothing to do with the periodic static charge distribution inside the bulk unit cell of the polarized solid.

So far, we have avoided any experimental consideration. How is \mathbf{P} measured? Certainly no one relies on measuring cell dipoles, although induced charge distributions of the kind shown in Fig. 2 are accessible to X-ray crystallography. A FE material sustains, by definition, a spontaneous macroscopic polarization, i.e., a nonvanishing value of \mathbf{P} in the absence of any perturbation. But once again, while the microscopic charge distribution inside the unit cell of a FE crystal is experimentally accessible, actual measurements of the spontaneous polarization are based on completely different ideas, more closely related to (5). As we will see below in Sect. 2, this approach defines the observable \mathbf{P} in a way that very naturally parallels experiments, both for spontaneous and induced polarization. We also see that the theory vindicates

the concept that macroscopic polarization is an intensive quantity, insensitive to surface effects, whose value is indeed determined by what “happens” in the bulk of the solid and not at its surface.

2 Polarization as an Adiabatic Flow of Current

2.1 How is Induced Polarization Measured?

Most measurements of bulk macroscopic polarization \mathbf{P} of materials do not access its absolute value, but only its derivatives, which are expressed as Cartesian tensors. For example, the permittivity

$$\chi_{\alpha\beta} = \frac{dP_\alpha}{d\mathcal{E}_\beta} \quad (6)$$

appearing in (1) is defined as the derivative of polarization with respect to field. Here, as throughout this chapter, Greek subscripts indicate Cartesian coordinates. Similarly, the pyroelectric coefficient

$$\Pi_\alpha = \frac{dP_\alpha}{dT}, \quad (7)$$

the piezoelectric tensor

$$\gamma_{\alpha\beta\delta} = \frac{\partial P_\alpha}{\partial \epsilon_{\beta\delta}} \quad (8)$$

of Sect. 4.3, and the dimensionless Born (or “dynamical” or “infrared”) charge

$$Z_{s,\alpha\beta}^* = \frac{\Omega}{e} \frac{\partial P_\alpha}{\partial u_{s,\beta}} \quad (9)$$

of Sect. 4.2, are defined in terms of derivatives with respect to temperature T , strain $\epsilon_{\beta\delta}$, and displacement \mathbf{u}_s of sublattice s , respectively. Here, $e > 0$ is the charge quantum, and from now on we use Ω to denote the primitive-cell volume V_{cell} . (In the above formulas, derivatives are to be taken at fixed electric field and fixed strain when these variables are not explicitly involved.)

We start by illustrating one such case, namely, piezoelectricity, in Fig. 3. The situation depicted in (a) is the one where (2) applies. Supposing that \mathbf{P} is zero in the unstrained state (e.g., by symmetry), then the piezoelectric constant is simply proportional to the value of \mathbf{P} in the final state. The disturbing feature is that piezoelectricity appears as a surface effect, and indeed the debate whether piezoelectricity is a bulk or a surface effect lasted in the literature until rather recently [10–16]. The modern theory parallels the situation depicted in (b) and provides further evidence that piezoelectricity is a bulk effect, if any was needed. While the crystal is strained, a transient

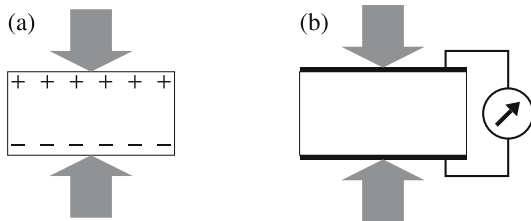


Fig. 3. Two possible realizations of the piezoelectric effect in a crystal strained along a piezoelectric axis. In (a) the crystal is not shorted, and induced charges pile up at its surfaces. Macroscopic polarization may be defined via (2), but the surface charges are an essential contribution to the integral. In (b) the crystal is inserted into a shorted capacitor; the surface charges are then removed by the electrodes, and the induced polarization is measured by the current flowing through the shorting wire

electrical current flows through the sample, and this is precisely the quantity being measured; the polarization of the final state is *not* obtained from a measurement performed on the final state only. In fact, the essential feature of (b) is its *time dependence*, although slow enough to ensure adiabaticity. The fundamental equation

$$\frac{d\mathbf{P}(t)}{dt} = \mathbf{j}(t), \quad (10)$$

where \mathbf{j} is the macroscopic (i.e., cell-averaged) current density, implies

$$\Delta\mathbf{P} = \mathbf{P}(\Delta t) - \mathbf{P}(0) = \int_0^{\Delta t} dt \mathbf{j}(t). \quad (11)$$

Notice that, in the adiabatic limit, \mathbf{j} goes to zero and Δt goes to infinity, while the integral in (11) stays finite. We also emphasize that currents are much easier to measure than dipoles or charges, and therefore (b), much more than (a), is representative of actual piezoelectric measurements.

At this point we return to the case of permittivity, i.e., polarization induced by an electric field, previously discussed in Sect. 1.1. It is expedient to examine Figs. 1 and 2 in a time-dependent way by imagining that the perturbing \mathcal{E} field is adiabatically switched on. There is then a transient macroscopic current flowing through the crystal cell, whose time-integrated value provides the induced macroscopic polarization, according to (11). This is true for both the CM case of Fig. 1 and the non-CM case of Fig. 2. The important difference is that in the former case the current displaces charge within each individual anion but vanishes on the cell boundary, while in the latter case the current flows throughout the interior of the crystal.

Using the examples of piezoelectricity and of permittivity, we have shown that the induced macroscopic polarization in condensed matter can be defined

and understood in terms of adiabatic flows of currents within the material. From this viewpoint, it becomes very clear how the value of \mathbf{P} is determined by what happens in the bulk of the solid, and why it is insensitive to surface effects.

2.2 How is Ferroelectric Polarization Measured?

FE materials are insulating solids characterized by a switchable macroscopic polarization \mathbf{P} . At equilibrium, a FE material displays a broken-symmetry, noncentrosymmetric structure, so that a generic vector property is not required to vanish by symmetry. The most important vector property is indeed \mathbf{P} , and its equilibrium value is known as the *spontaneous polarization*.

However, the value of \mathbf{P} is never measured directly as an equilibrium property; instead, all practical measurements exploit the switchability of \mathbf{P} . In most crystalline FEs, the different structures are symmetry-equivalent; that is, the allowed values of \mathbf{P} are equal in modulus and point along equivalent (enantiomorphous) symmetry directions. In a typical experiment, application of a sufficiently strong electric field switches the polarization from \mathbf{P} to $-\mathbf{P}$, so that one speaks of polarization *reversal*.

The quantity directly measured in a polarization-reversal experiment is the difference in polarization between the two enantiomorphous structures; making use of symmetry, one can then equate this difference to twice the spontaneous polarization. This pragmatic working definition of spontaneous polarization has, as a practical matter, been adopted by the experimental community since the early days of the field. However, it was generally considered that this was done only as an expedient, because direct access to the “polarization itself” was difficult to obtain experimentally. Instead, with the development of modern electronic-structure methods and the application of these methods to FE materials, it became evident that the previous “text-book definitions” [7, 8] of \mathbf{P} were also unworkable from the *theoretical* point of view. It was found that such attempts to define \mathbf{P} as a single-valued equilibrium property of the crystal in a given broken-symmetry state, in the spirit of (3), were doomed to failure because they could not be implemented in an unambiguous way.

In response to this impasse, a new theoretical viewpoint emerged in the early 1990s and was instrumental in the development of a successful microscopic theory [17–19]. As we shall see, this modern theory of polarization actually elevates the old pragmatic viewpoint to the status of a postulate. Rather than focusing on \mathbf{P} as an equilibrium property of the crystal in a given state, one focuses on *differences* in polarization between two different states [17]. From the theoretical viewpoint, this represents a genuine change of paradigm, albeit one that is actually harmonious with the old experimental pragmatism.

We illustrate a polarization-reversal experiment by considering the case of the perovskite oxide PbTiO_3 , whose equilibrium structure at zero temper-

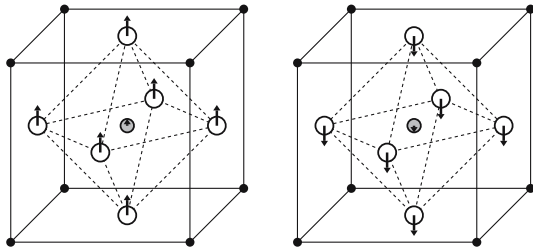


Fig. 4. Tetragonal structure of PbTiO_3 : solid, shaded, and empty circles represent Pb, Ti, and O atoms, respectively. The arrows indicate the actual magnitude of the atomic displacements, where the origin has been kept at the Pb site (the Ti displacements are barely visible). Two enantiomorphous structures, with polarization along $[001]$, are shown here. Application of a large enough electric field (coercive field) switches between the two and reverses the polarization

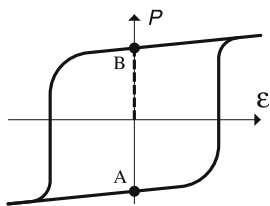


Fig. 5. A typical hysteresis loop; the magnitude of the spontaneous polarization is also shown (*vertical dashed segment*). Notice that spontaneous polarization is a zero-field property

ature is tetragonal. There are six enantiomorphous broken-symmetry structures; two of them, having opposite nuclear displacements and opposite values of \mathbf{P} , are shown in Fig. 4.

A typical measurement of the spontaneous polarization, performed through polarization reversal, is schematically shown in Fig. 5. The hysteresis cycle is in fact the primary experimental output. The transition between the two enantiomorphous FE structures A and B of Fig. 4 is driven by an applied electric field; the experimental setup typically measures the integrated macroscopic current flowing through the sample, as in (11). One half of the difference $\mathbf{P}_B - \mathbf{P}_A$ defines the magnitude \mathbf{P}_s of the spontaneous polarization in the vertical direction. From Fig. 5, it is clear that \mathbf{P}_s can also be defined as the polarization difference $\Delta\mathbf{P}$ between the broken-symmetry B structure and the centrosymmetric structure (where the displacements are set to zero). Notice that, while a field is needed to induce the switching in the actual experiment, ideally one could evaluate $\Delta\mathbf{P}$ along the vertical axis in Fig. 5, where the macroscopic field is identically zero. We stress that the experiment measures neither \mathbf{P}_A nor \mathbf{P}_B , but only their *difference*. It is only an additional symmetry argument that allows one to infer the value of each of them from the actual experimental data.

2.3 Basic Prescriptions for a Theory of Polarization

For both induced and spontaneous polarization, we have emphasized the role of adiabatic currents in order to arrive at a microscopic theory of \mathbf{P} , which by construction must be an intensive bulk property, insensitive to the boundaries. The root of this theory is in (11), whose form we simplify by introducing a parameter λ having the meaning of a dimensionless adiabatic time: λ varies continuously from zero (corresponding to the initial system) to 1 (corresponding to the final system). Then we can write (11) as

$$\Delta\mathbf{P} = \int_0^1 d\lambda \frac{d\mathbf{P}}{d\lambda}. \quad (12)$$

In general, “initial” and “final” refer to the state of the system before and after the application of some slow sublattice displacements, strains, electric fields, etc. The key feature exploited here is that $d\mathbf{P}/d\lambda$ is a well-defined bulk vector property. We notice, however, that an important condition for (12) to hold is that the system remain insulating for all intermediate values of λ , since the transient current is otherwise *not* uniquely defined. Note that for access to the response properties of (6)–(9), no integration is needed; the physical quantity of interest coincides by definition with $d\mathbf{P}/d\lambda$ evaluated at an appropriate λ .

In order to focus the discussion onto the spontaneous polarization of a FE, we now let λ scale the sublattice displacements (the lengths of the arrows in Fig. 4) leading from a centrosymmetric reference structure ($\lambda = 0$) to the spontaneously polarized structure ($\lambda = 1$). Then the spontaneous polarization may be written [17]

$$\mathbf{P}_{\text{eff}} = \int_0^1 d\lambda \frac{d\mathbf{P}}{d\lambda} \quad (\lambda = 0 : \text{centrosymmetric reference}). \quad (13)$$

For later reference, note that this is the “effective” and not the “formal” definition of polarization as given later in (20) and discussed in the later parts of Sect. 3.

The current-carrying particles are electrons and nuclei; while the quantum nature of the former is essential, the latter can be safely dealt with as classical point charges, whose current contributions to (11) and to (12) are trivial. We focus then mostly on the electronic term in the currents and in \mathbf{P} , although it has to be kept in mind that the overall charge neutrality of the condensed system is essential. Furthermore, from now on we limit ourselves to a zero-temperature framework, thus ruling out the phenomenon of pyroelectricity.

We refer, once more, to Fig. 2, where the quantum nature of the electrons is fully accounted for. As explained above, in order to obtain \mathbf{P} via (11), one needs the adiabatic electronic current that flows through the crystal while the perturbation is switched on. Within a quantum-mechanical description of the electronic system, currents are closely related to the *phase* of the wavefunction

(for instance, if the wavefunction is real, the current vanishes everywhere). But only the *modulus* of the wavefunction has been used in drawing the charge distribution of Fig. 2; any phase information has been obliterated, so that the value of \mathbf{P} cannot be retrieved. Interestingly, this argument is in agreement with the general concept, strongly emphasized above, that the periodic polarization charge inside the material has nothing to do with the value of macroscopic polarization.

Next, it is expedient to discuss a little more thoroughly the role of the electric field \mathcal{E} . A direct treatment of a finite electric field is subtle, because the periodicity of the crystal Hamiltonian, on which the Bloch theorem depends, is absent unless \mathcal{E} vanishes (see Sect. 5.1). However, while \mathcal{E} is by definition the source inducing \mathbf{P} in the case of permittivity in (6), a source *other* than the electric field is involved in the cases of pyroelectricity (7), piezoelectricity (8), dynamical effective charges (9), and spontaneous polarization (13). While it is sometimes appropriate to take these latter derivatives under electrical boundary conditions other than those of a vanishing field, we shall restrict ourselves here to the most convenient and fundamental definitions in which the field \mathcal{E} is set to zero. For example, piezoelectricity, when measured as in Fig. 3b, is clearly a zero-field property, since the sample is shorted at all times. Spontaneous polarization, when measured as in Fig. 5, is obviously a zero-field property as well. Born effective charges, which will be addressed below, are also defined as zero-field tensors. Then, as an example of two different choices of boundary conditions to address the same phenomenon, we may consider again the case of piezoelectricity, Fig. 3. While in Fig. 3b the field is zero, in Fig. 3a a nonvanishing (“depolarizing”) field is clearly present inside the material. The two piezoelectric tensors, phenomenologically defined in these two different ways, are not equal but are related in a simple way (in fact, they are proportional via the dielectric tensor).

Thus, it is possible to access many of the interesting physical properties, including piezoelectricity, lattice dynamics, and ferroelectricity, with calculations performed at zero field. We will restrict ourselves to this case for most of this chapter. As for the permittivity, it is theoretically accessible by means of either the linear-response theory (see [20] for a thorough review), or via an extension of the Berry-phase theory to finite electric field that will be described briefly in Sect. 5.1.

3 Formal Description of the Berry-Phase Theory

In this section, we shall give an introduction to the modern theory of polarization that was developed in the 1990s. Following important preliminary developments of *Resta* [17], the principal development of the theory was introduced by *King-Smith* and *Vanderbilt* [18] and soon afterwards reviewed by *Resta* [19]. This theory is sometimes known as the “Berry-phase theory of

polarization” because the polarization is expressed in the form of a certain quantum phase known as a Berry phase [21, 22].

In order to deal with macroscopic systems, both crystalline and disordered, it is almost mandatory in condensed-matter theory to assume periodic (Born–von Kármán) boundary conditions [7, 8]. This amounts to considering the system in a finite box that is periodically repeated, in a ring-like fashion, in all three Cartesian directions. Eventually, the limit of an infinitely large box is taken. For practical purposes, the thermodynamic limit is approached when the box size is much larger than a typical atomic dimension. Among other features, a system of this kind has no surface and all of its properties are by construction “bulk” ones. When the system under consideration is a many-electron system, the periodic boundary conditions amount to requiring that the wavefunction and the Hamiltonian be periodic over the box. As indicated previously, our discussion will be restricted to the case of vanishing electric field unless otherwise stated.

We give below only a brief sketch of the derivation of the central formulas of the theory; interested readers are referred to [18, 19, 23] for details.

3.1 Formulation in Continuous k -Space

If we adopt for the many-electron system a mean-field treatment, such as the Kohn–Sham one [5], the self-consistent one-body potential is periodic over the Born–von Kármán box, provided the electric field \mathcal{E} vanishes, for any value of the parameter λ . Furthermore, if we consider a *crystalline* system, the self-consistent potential also has the lattice periodicity. The eigenfunctions are of the Bloch form $\psi_{n\mathbf{k}}(\mathbf{r}) = e^{i\mathbf{k}\cdot\mathbf{r}} u_{n\mathbf{k}}(\mathbf{r})$, where u is lattice-periodical, and obey the Schrödinger equation $H|\psi_{n\mathbf{k}}\rangle = E_{n\mathbf{k}}|\psi_{n\mathbf{k}}\rangle$, where $H = p^2/2m + V$. Equivalently, the eigenvalue problem can be written as $H_{\mathbf{k}}|u_{n\mathbf{k}}\rangle = E_{n\mathbf{k}}|u_{n\mathbf{k}}\rangle$, where

$$H_{\mathbf{k}} = \frac{(\mathbf{p} + \hbar\mathbf{k})^2}{2m} + V. \quad (14)$$

All of these quantities depend implicitly on a parameter λ that changes slowly in time, such that the wavefunction acquires, from elementary adiabatic perturbation theory, a first-order correction

$$|\delta\psi_{n\mathbf{k}}\rangle = -i\hbar\dot{\lambda} \sum_{m \neq n} \frac{\langle\psi_{m\mathbf{k}}|\partial_{\lambda}\psi_{n\mathbf{k}}\rangle}{E_{n\mathbf{k}} - E_{m\mathbf{k}}} |\psi_{m\mathbf{k}}\rangle, \quad (15)$$

where $\dot{\lambda} = d\lambda/dt$ and ∂_λ is the derivative with respect to the parameter λ . The corresponding first-order current arising from the entire band n is then¹

$$\mathbf{j}_n = \frac{d\mathbf{P}_n}{dt} = \frac{i\hbar e\dot{\lambda}}{(2\pi)^3 m} \sum_{m \neq n} \int d\mathbf{k} \frac{\langle \psi_{n\mathbf{k}} | \mathbf{p} | \psi_{m\mathbf{k}} \rangle \langle \psi_{m\mathbf{k}} | \partial_\lambda \psi_{n\mathbf{k}} \rangle}{E_{n\mathbf{k}} - E_{m\mathbf{k}}} + \text{c.c.}, \quad (16)$$

where ‘‘c.c.’’ denotes the complex conjugate. Time t can be eliminated by removing $\dot{\lambda}$ from the right-hand side and replacing $d\mathbf{P}/dt \rightarrow d\mathbf{P}/d\lambda$ on the left-hand side above. Then, making use of ordinary perturbation theory applied to the dependence of $H_{\mathbf{k}}$ in (14) upon \mathbf{k} , one obtains, after some manipulation,

$$\frac{d\mathbf{P}_n}{d\lambda} = \frac{ie}{(2\pi)^3} \int d\mathbf{k} \langle \nabla_{\mathbf{k}} u_{n\mathbf{k}} | \partial_\lambda u_{n\mathbf{k}} \rangle + \text{c.c.}. \quad (17)$$

It is noteworthy that the sum over ‘‘unoccupied’’ states m has disappeared from this formula, corresponding to our intuition that the polarization is a ground-state property. Summing now over the occupied states, and inserting in (12), we get the spontaneous polarization of a FE. The result, after an integration with respect to λ , is that the effective polarization (13) takes the form

$$\mathbf{P}_{\text{eff}} = \Delta \mathbf{P}_{\text{ion}} + [\mathbf{P}_{\text{el}}(1) - \mathbf{P}_{\text{el}}(0)], \quad (18)$$

where the nuclear contribution $\Delta \mathbf{P}_{\text{ion}}$ has been restored, and

$$\mathbf{P}_{\text{el}}(\lambda) = \frac{e}{(2\pi)^3} \Im \sum_n \int d\mathbf{k} \langle u_{n\mathbf{k}} | \nabla_{\mathbf{k}} | u_{n\mathbf{k}} \rangle. \quad (19)$$

Here, the sum is over the occupied states, and $|u_{n\mathbf{k}}\rangle$ are understood to be implicit functions of λ . In the case that the adiabatic path takes a FE crystal from its centrosymmetric reference state to its equilibrium polarized state, \mathbf{P}_{eff} of (18) is just exactly the spontaneous polarization.

Equation (19) is the central result of the modern theory of polarization. Those familiar with Berry-phase theory [21, 22] will recognize $\mathbf{A}(\mathbf{k}) = i\langle u_{n\mathbf{k}} | \nabla_{\mathbf{k}} | u_{n\mathbf{k}} \rangle$ as a ‘‘Berry connection’’ or ‘‘gauge potential’’; its integral over a closed manifold (here the Brillouin zone) is known as a ‘‘Berry phase’’. It is remarkable that the result (19) is independent of the path traversed through parameter space (and of the rate of traversal, as long as it is adiabatically slow), so that the result depends only on the endpoints. Implicit in the analysis is that the system must remain insulating everywhere along the path, as otherwise the adiabatic condition fails.

¹ In this and subsequent formulas, we assume that n is really a composite index for band and spin. Alternatively, factors of two may be inserted into the equations to account for spin degeneracy.

To obtain the total polarization, the ionic contribution must be added to (19). The total polarization is then $\mathbf{P} = \mathbf{P}_{\text{el}} + \mathbf{P}_{\text{ion}}$ or

$$\mathbf{P} = \frac{e}{(2\pi)^3} \Im \sum_n \int d\mathbf{k} \langle u_{n\mathbf{k}} | \nabla_{\mathbf{k}} | u_{n\mathbf{k}} \rangle + \frac{e}{\Omega} \sum_s Z_s^{\text{ion}} \mathbf{r}_s, \quad (20)$$

where the first term is (19) and the second is \mathbf{P}_{ion} , the contribution arising from positive point charges eZ_s^{ion} located at atomic positions \mathbf{r}_s . In principle, the band index n should run over all bands, including those made from core states, and Z^{ion} should be the bare nuclear charge. However, in the frozen-core approximation that underlies pseudopotential theory, we let n run over valence bands only, and Z^{ion} is the net positive charge of the nucleus plus core. We adopt the latter interpretation here.

We refer to the polarization of (20) as the ‘‘formal polarization’’ to distinguish it from the ‘‘effective polarization’’ of (13) or (18). The two definitions coincide only if the formal polarization vanishes for the centrosymmetric reference structure used to define \mathbf{P}_{eff} , which, as we shall see in Sect. 3.4, need not be the case.

3.2 Formulation in Discrete k -Space

In practical numerical calculations, equations such as (16), (17), and (19) are summed over a discrete mesh of \mathbf{k} -points spanning the Brillouin zone. Since the $\nabla_{\mathbf{k}}$ operator is a derivative in \mathbf{k} -space, its finite-difference representation will involve couplings between neighboring points in \mathbf{k} -space.

For pedagogic purposes, we illustrate this by starting from the one-dimensional version of (19), namely, $P_n = (e/2\pi) \varphi_n$, where

$$\varphi_n = \Im \int dk \langle u_{nk} | \partial_k | u_{nk} \rangle, \quad (21)$$

and note that this can be discretized as

$$\varphi_n = \Im \ln \prod_{j=0}^{M-1} \langle u_{n,k_j} | u_{n,k_{j+1}} \rangle, \quad (22)$$

where $k_j = 2\pi j/Ma$ is the j th k -point in the Brillouin zone. This follows by inserting the expansion $u_{n,k+dk} = u_{nk} + dk (\partial_k u_{nk}) + \mathcal{O}(dk^2)$ into (21) and keeping the leading term.

In (22), it is understood that the wavefunctions at the boundary points of the Brillouin zone are related by $\psi_{n,0} = \psi_{n,2\pi/a}$, so that

$$u_{n,k_0}(x) = e^{2\pi i x/a} u_{n,k_M}(x) \quad (23)$$

and there are only M independent states u_{n,k_0} to $u_{n,k_{M-1}}$. Thus, it is natural to regard the Brillouin zone as a *closed space* (in 1D, a loop) as illustrated in Fig. 6.

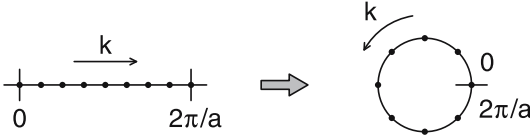


Fig. 6. Illustration showing how the Brillouin zone in one dimension (*left*) can be mapped onto a circle (*right*), in view of the fact that wavevectors $k = 0$ and $k = 2\pi/a$ label the same states

Equation (22) makes it easy to see why this quantity is called a Berry “phase”. We are instructed to compute the global product of wavefunctions

$$\dots \langle u_{k_1} | u_{k_2} \rangle \langle u_{k_2} | u_{k_3} \rangle \langle u_{k_3} | u_{k_4} \rangle \dots \quad (24)$$

across the Brillouin zone, which in general is a complex number; then the operation “ $\Im \ln$ ” takes the phase of this number. Note that this global phase is actually insensitive to a change of the phase of any one wavefunction u_k , since each u_k appears once in a bra and once in a ket. We can thus view the “Berry phase” φ_n , giving the contribution to the polarization arising from band n , as a global phase property of the manifold of occupied one-electron states.

In three dimensions (3D), the Brillouin zone can be regarded as a closed 3-torus obtained by identifying boundary points $\psi_{n\mathbf{k}} = \psi_{n,\mathbf{k}+\mathbf{G}_j}$, where \mathbf{G}_j is a primitive reciprocal lattice vector. The Berry phase for band n in direction j is $\varphi_{n,j} = (\Omega/e) \mathbf{G}_j \cdot \mathbf{P}_n$, where \mathbf{P}_n is the contribution to (19) from band n , so that

$$\varphi_{n,j} = \Omega_{\text{BZ}}^{-1} \Im \int_{\text{BZ}} d^3k \langle u_{n\mathbf{k}} | \mathbf{G}_j \cdot \nabla_{\mathbf{k}} | u_{n\mathbf{k}} \rangle. \quad (25)$$

We then have

$$\mathbf{P}_n = \frac{1}{2\pi} \frac{e}{\Omega} \sum_j \varphi_{n,j} \mathbf{R}_j, \quad (26)$$

where \mathbf{R}_j is the real-space primitive translation corresponding to \mathbf{G}_j . To compute the $\varphi_{n,j}$ for a given direction j , the sampling of the Brillouin zone is arranged as in Fig. 7, where k_{\parallel} is the direction along \mathbf{G}_j and \mathbf{k}_{\perp} refers to the 2D space of wavevectors spanning the other two primitive reciprocal lattice vectors. For a given \mathbf{k}_{\perp} , the Berry phase $\varphi_{n,j}(\mathbf{k}_{\perp})$ is computed along the string of M k -points extending along k_{\parallel} as in (22), and finally a conventional average over the \mathbf{k}_{\perp} is taken:

$$\varphi_{n,j} = \frac{1}{N_{\mathbf{k}_{\perp}}} \sum_{\mathbf{k}_{\perp}} \varphi_n(\mathbf{k}_{\perp}). \quad (27)$$

Note that a subtlety arises in regard to the “choice of branch” when taking this average, as discussed in the next subsection. Moreover, in 3D crystals,

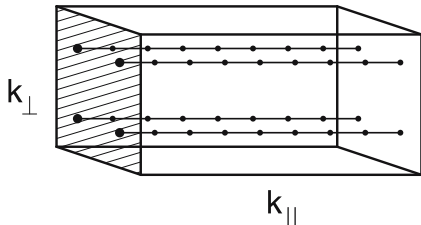


Fig. 7. Arrangement of Brillouin zone for computation of component of \mathbf{P} along k_{\parallel} direction

it may happen that some groups of bands must be treated using a many-band generalization of (22) due to degeneracy at high-symmetry points in the Brillouin zone; see [18, 19] for details.

The computation of \mathbf{P} according to (26) is now a standard option in several popular electronic-structure codes (ABINIT², CRYSTAL³, PWSCF⁴, SIESTA⁵, and VASP⁶).

3.3 The Quantum of Polarization

It is clear that (22), being a phase, is only well-defined mod 2π . We can see this more explicitly in (21); let

$$|\tilde{u}_{nk}\rangle = e^{-i\beta(k)} |u_{nk}\rangle \quad (28)$$

be a new set of Bloch eigenstates differing only in the choice of phase as a function of k . Here $\beta(k)$ is real and obeys $\beta(2\pi/a) - \beta(0) = 2\pi m$, where m is an integer, in order that $\tilde{\psi}_{n,0} = \tilde{\psi}_{n,2\pi/a}$. Then inserting into (22) we find that

$$\tilde{\varphi}_n = \varphi_n + \int_0^{2\pi/a} dk \left(\frac{d\beta}{dk} \right) dk = \varphi_n + 2\pi m. \quad (29)$$

Thus, φ_n is really only well-defined “mod 2π ”.

In view of this uncertainty, care must be taken in the 3D case when averaging $\varphi_n(\mathbf{k}_{\perp})$ over the 2D Brillouin zone of \mathbf{k}_{\perp} space: the choice of branch cut must be made in such a way that $\varphi_n(\mathbf{k}_{\perp})$ remains continuous in \mathbf{k}_{\perp} . In practice, a conventional mesh sampling is used in the \mathbf{k}_{\perp} space, and the average is computed as in (27). Consider, for example, Fig. 7, where $N_{\mathbf{k}_{\perp}} = 4$. If the branch cut is chosen independently for each \mathbf{k}_{\perp} so as to map $\varphi_n(\mathbf{k}_{\perp})$ to the interval $[-\pi, \pi]$, and if the four values were found to be 0.75π , 0.85π , 0.95π , and -0.95π , then the last value must be remapped to become 1.05π

² <http://www.abinit.org/>

³ <http://www.crystal.unito.it/>

⁴ <http://www.pwscf.org>

⁵ <http://www.uam.es/departamentos/ciencias/fismateriac/siesta>

⁶ <http://cms.mpi.univie.ac.at/vasp/>

before the average is taken in (27). That is, the correct average is 0.90π , or equivalently -1.10π , but *not* 0.40π as would be obtained by taking the average blindly.

In other words, care must be taken to make a *consistent* choice of phases on the right-hand side of (27). However, it is still permissible to shift all of the $N_{\mathbf{k}_\perp}$ phases by a common amount $2\pi m_j$. Thus, each $\varphi_{n,j}$ in (26) is only well-defined mod 2π , leading to the conclusion that \mathbf{P}_n is only well-defined mod $e\mathbf{R}/\Omega$, where $\mathbf{R} = \sum_j m_j \mathbf{R}_j$ is a lattice vector. The same conclusion results from generalizing the argument of (28) and (29) to 3D, showing that a phase twist of the form $|\tilde{u}_{n\mathbf{k}}\rangle = \exp[-i\beta(\mathbf{k})]|u_{n\mathbf{k}}\rangle$ results in

$$\tilde{\mathbf{P}}_n = \mathbf{P}_n + \frac{e\mathbf{R}}{\Omega}, \quad (30)$$

where \mathbf{R} is a lattice vector.

These arguments are for a single band, but the same obviously applies to the sum over all occupied bands. *We thus arrive at a central result of the modern theory of polarization:* the formal polarization, defined via (20) or calculated through (26), is *only well-defined mod $e\mathbf{R}/\Omega$* , where \mathbf{R} is any lattice vector and Ω is the primitive-cell volume.

At first sight the presence of this uncertainty modulo the quantum $e\mathbf{R}/\Omega$ may be surprising, but in retrospect it should have been expected. Indeed, the ionic contribution given by the second term of (20) is subject to precisely the same uncertainty, arising from the arbitrariness of the nuclear location \mathbf{r}_s modulo a lattice vector \mathbf{R} . The choice of one particular value of \mathbf{P} from among the lattice of values related to each other by addition of $e\mathbf{R}/\Omega$ will be referred to as the “choice of branch”.

Summarizing our results so far, we find that the *formal polarization* \mathbf{P} , defined by (20), is only well-defined mod $e\mathbf{R}/\Omega$, where \mathbf{R} is any lattice vector. Moreover, we have found that the change in polarization $\Delta\mathbf{P}$ along an adiabatic path, as defined by (12), is connected with this formal polarization by the relation

$$\Delta\mathbf{P} := (\mathbf{P}_{\lambda=1} - \mathbf{P}_{\lambda=0}) \bmod \frac{e\mathbf{R}}{\Omega}. \quad (31)$$

This central formula, embodying the main content of the modern theory of polarization, requires careful explanation. For a given adiabatic path, the change in polarization appearing on the left-hand side of (31), and defined by (12), is given by a single-valued vector quantity that is perfectly well defined and has no “modulus” uncertainty. On the right-hand side, $\mathbf{P}_{\lambda=0}$ and $\mathbf{P}_{\lambda=1}$ are, respectively, the formal polarization of (20) evaluated at the start and end of the path. The symbol “:=” has been introduced to indicate that the value on the left-hand side is equal to one of the values on the right-hand side. Thus, the precise meaning of (31) is that the actual integrated adiabatic current flow $\Delta\mathbf{P}$ is equal to $(\mathbf{P}_{\lambda=1} - \mathbf{P}_{\lambda=0}) + e\mathbf{R}/\Omega$ for some lattice vector \mathbf{R} .

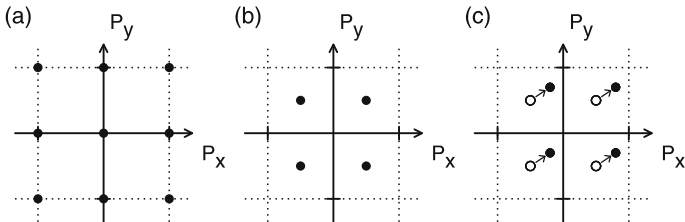


Fig. 8. Polarization as a lattice-valued quantity, illustrated for a 2D square-lattice system. Here, (a) and (b) illustrate the two possible states of polarization consistent with full square-lattice symmetry, while (c) illustrates a possible change in polarization induced by some symmetry-lowering change of the Hamiltonian. In (c), the arrows show the “effective polarization” as defined in (13)

It follows that (31) cannot be used to determine $\Delta\mathbf{P}$ completely; it only determines $\Delta\mathbf{P}$ within the same uncertainty mod $e\mathbf{R}/\Omega$ that applies to \mathbf{P}_λ . Fortunately, the typical magnitude of \mathbf{P}_{eff} , and of polarization differences in general, is small compared to this “quantum”. For cubic perovskites, $a \simeq 4 \text{ \AA}$, so that the effective quantum for spin-paired systems is $2e/a^2 \simeq 2.0 \text{ C/m}^2$. In comparison, the spontaneous polarization of perovskite ferroelectrics is typically in the range of about 0.3 to 0.6 C/m^2 , significantly less than this quantum. Thus, this uncertainty mod $e\mathbf{R}/\Omega$ is rarely a serious concern in practice. If there is doubt about the correct choice of branch for a given path, this doubt can usually be resolved promptly by computing the polarization at several intermediate points along the path; as long as $\Delta\mathbf{P}$ is small for each step along the path, the correct interpretation of the evolution of the polarization will be clear.

3.4 Formal Polarization as a Multivalued Vector Quantity

A useful way to think about the presence of this “modulus” is to regard the formal polarization as a *multivalued vector quantity*, rather than a conventional single-valued one. That is, the question “What is \mathbf{P} ?” is answered not by giving a single vector, but a lattice of vector values related by translations $e\mathbf{R}/\Omega$. Here, we explain how this viewpoint contributes to an understanding of the role of symmetry and provides an alternative perspective on the central result (31) of the previous subsection.

Let us begin with symmetry considerations, where we find some surprising results. Consider, for example, KNbO_3 in its ideal cubic structure. Because of the cubic symmetry, one might expect that \mathbf{P} as calculated from (20) would vanish; or more precisely, given the uncertainty expressed by (30), that it would take on a lattice of values $(m_1, m_2, m_3)e/a^2$ that includes the zero vector (m_j are integers). This expected situation is sketched (in simplified 2D form) in Fig. 8a.

Table 1. Atomic positions $\boldsymbol{\tau}$ and nominal ionic charges Z for KNbO_3 in its centrosymmetric cubic structure with lattice constant a

Atom	τ_x	τ_y	τ_z	Z^{ion}
K	0	0	0	+1
Nb	$a/2$	$a/2$	$a/2$	+5
O ₁	0	$a/2$	$a/2$	-2
O ₂	$a/2$	0	$a/2$	-2
O ₃	$a/2$	$a/2$	0	-2

However, when the result is actually calculated from (20) using first-principles electronic-structure methods, *this is not what one finds*. Instead, one finds that

$$\mathbf{P} = \left(m_1 + \frac{1}{2}, m_2 + \frac{1}{2}, m_3 + \frac{1}{2} \right) \frac{e}{a^2} \quad (\text{integer } m_j), \quad (32)$$

which is indeed a multivalued object, but corresponding to the situation sketched in Fig. 8b, not Fig. 8a!

While this result emerges above from a fully quantum-mechanical calculation, it is not essentially a quantum-mechanical result. Indeed, it could have been anticipated based on purely classical arguments as applied to an ideal ionic model of the KNbO_3 crystal. In such a picture, the formal polarization is written as

$$\mathbf{P} = \frac{e}{\Omega} \sum_s Z_s^{\text{ion}} \boldsymbol{\tau}_s, \quad (33)$$

where $\boldsymbol{\tau}_s$ is the location, and Z_s^{ion} is the nominal (integer) ionic charge, of ion s . Evaluating (33) using the values given in Table 1 yields $\mathbf{P} = (\frac{1}{2}, \frac{1}{2}, \frac{1}{2})e/a^2$. However, each vector $\boldsymbol{\tau}_s$ is arbitrary modulo a lattice vector. For example, it is equally valid to replace $\boldsymbol{\tau}_{\text{K}} = (0, 0, 0)$ by $\boldsymbol{\tau}_{\text{K}} = (a, a, a)$, yielding $\mathbf{P} = (\frac{3}{2}, \frac{3}{2}, \frac{3}{2})e/a^2$, which is again consistent with (32). Similarly, since each Z_s^{ion} is an integer,⁷ the shift of any $\boldsymbol{\tau}_s$ by a lattice vector $\Delta\mathbf{R}$ simply generates a shift to one of the other vectors on the right-hand side of (32). This heuristic ionic model then leads to the same conclusion expressed in (32), i.e., that Fig. 8b and not Fig. 8a is appropriate for the case of cubic KNbO_3 .

This may appear to be a startling result. We are saying that the polarization as defined by (20) does not necessarily vanish for a centrosymmetric structure (or more precisely, that the lattice of values corresponding to \mathbf{P} does not contain the zero vector). Is this in conflict with the usual observation that

⁷ For precisely this reason, it is necessary to use an ionic model with formal integer ionic charges for arguments of this kind. This requirement can be justified using arguments based on a Wannier representation.

a vector-valued physical quantity must vanish in a centrosymmetric crystal? No, because this theorem applies only to a normal (that is, single-valued) vector quantity. Instead, *the formal polarization is a multivalued vector quantity*. The constraint of centrosymmetry requires that the polarization must get mapped onto itself by the inversion operation. This would be impossible for a nonzero single-valued vector, but it *is* possible for a lattice of vector values, as illustrated in Fig. 8b. Indeed, the lattice of values shown in Fig. 8b is invariant with respect to all the operations of the cubic symmetry group, as are those of Fig. 8a. Actually, for a simple cubic structure with full cubic symmetry, these are the *only two possibilities* consistent with symmetry. It is not possible to know, from symmetry alone, which of these representations of the formal polarization is correct. A heuristic argument of the kind leading to (32) can be used to guess the correct result, but it should be confirmed by actual calculation. The heuristic arguments suggest, and first-principles calculations confirm, that the formal polarizations of BaTiO₃ and KNbO₃ are not equal, even though they have identical symmetry; they correspond to Fig. 8a and Fig. 8b, respectively!

How should we understand the spontaneous polarization \mathbf{P}_s of ferroelectrically distorted KNbO₃ in the present context? Recall that \mathbf{P}_s is defined as the effective polarization \mathbf{P}_{eff} of (13) for the case of an adiabatic path carrying KNbO₃ from its unstable cubic to its relaxed FE structure. Suppose that one were to find that this adiabatic evolution carried the polarization along the path indicated by the arrows in Fig. 8c. In this case, the effective polarization \mathbf{P}_{eff} of (13) is definitely known to correspond to the vector sketched repeatedly in Fig. 8c. However, when one evaluates $\Delta\mathbf{P}$ from (31), using only a knowledge of the endpoints of the path, the knowledge of the correct branch is lost. For example, one could not be certain that the actual $\Delta\mathbf{P}$ associated with this path is the one shown in Fig. 8c, rather than one pointing from an open circle in one cell to a closed one in a neighboring cell (and differing by the “modulus” $e\mathbf{R}/\Omega$). This is, of course, just the same uncertainty attached to (31) and discussed in detail in the previous subsection, now expressed from a more graphical point of view.

3.5 Mapping onto Wannier Centers

Another way of thinking about the meaning of the Berry-phase polarization, and of the indeterminacy of the polarization modulo the quantum $e\mathbf{R}/\Omega$, is in terms of Wannier functions. The Wannier functions are localized functions $w_{n\mathbf{R}}(\mathbf{r})$, labeled by band n and unit cell \mathbf{R} , that span the same Hilbert subspace as do the Bloch states $|\psi_{n\mathbf{k}}\rangle$. In fact, they are connected by a Fourier-transform-like expression

$$|w_{n\mathbf{R}}\rangle = \frac{\Omega}{(2\pi)^3} \int d\mathbf{k} e^{i\mathbf{k}\cdot\mathbf{R}} |\psi_{n\mathbf{k}}\rangle, \quad (34)$$

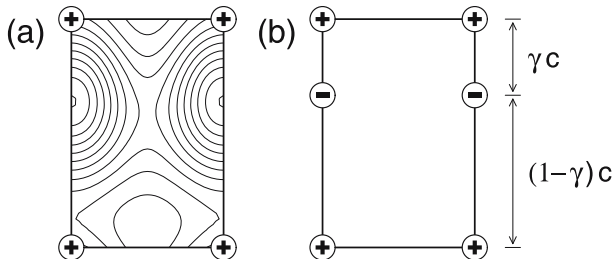


Fig. 9. Illustrative tetragonal crystal (cell dimensions $a \times a \times c$) having one mono-valent ion at the cell corner (origin) and one occupied valence band. (a) The distributed quantum-mechanical charge distribution associated with the electron band, represented as a contour plot. (b) The distributed electron distribution has been replaced by a unit point charge $-e$ located at the Wannier center \mathbf{r}_n , as given by the Berry-phase theory

where the Bloch states are normalized to unity over the crystal cell. Once we have the Wannier functions, we can locate the “Wannier centers” $\mathbf{r}_{n\mathbf{R}} = \langle w_{n\mathbf{R}} | \mathbf{r} | w_{n\mathbf{R}} \rangle$. It turns out that the location of the Wannier center is simply

$$\mathbf{r}_{n\mathbf{R}} = \frac{\Omega}{e} \mathbf{P}_n + \mathbf{R}. \quad (35)$$

That is, specifying the contribution of band n to the Berry-phase polarization is really just equivalent to specifying the location of the Wannier center in the unit cell. Because the latter is indeterminate mod \mathbf{R} , the former is indeterminate mod $e\mathbf{R}/\Omega$.

Thus, the Berry-phase theory can be regarded as providing a mapping of the distributed quantum-mechanical electronic charge density onto a lattice of negative point charges of charge $-e$, as illustrated in Fig. 9. While the CM picture obviously *cannot* be applied to the situation of Fig. 9a, because the charge density vanishes nowhere in the unit cell, it *can* be applied to the situation of Fig. 9b without problem. The only question is whether the negative charge located at $z = (1 - \gamma)c$ in this figure should be regarded as “living” in the same unit cell as the positive nucleus at the origin or the one at $z = c$; this uncertainty corresponds precisely to the “quantum of polarization” $e\mathbf{R}/\Omega$ for the case $\mathbf{R} = c\hat{z}$.

It therefore appears that, by adopting the Wannier-center mapping, the CM viewpoint has been rescued. We are in fact decomposing the charge (nuclear and electronic) into localized contributions whose dipoles determine \mathbf{P} . However, one has to bear in mind that the *phase* of the Bloch orbitals is essential to actually perform the Wannier transformation. Knowledge of their *modulus* is not enough, while we stress once more that the modulus uniquely determines the periodic polarization charge, such as the one shown in Fig. 9a.

Before leaving this discussion, it is amusing to consider the behavior of the Wannier centers \mathbf{r}_n under a *cyclic* adiabatic evolution of the Hamiltonian.

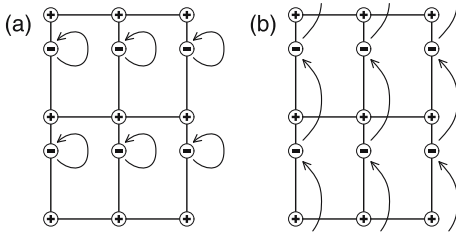


Fig. 10. Possible evolution of positions of Wannier centers ($-$), relative to the lattice of ions ($+$), as the Hamiltonian evolves adiabatically around a closed loop. Wannier functions must return to themselves, but can do so either (a) without, or (b) with, a coherent shift by a lattice vector

That is, we want to integrate the net adiabatic current flow as the system is taken around a *closed loop* in some multidimensional parameter space. (For example, one atomic sublattice might be displaced by 0.1 \AA first along $+\hat{x}$, then $+\hat{y}$, then $-\hat{x}$, and then $-\hat{y}$.) Referring to (12) and (13), we have for this case

$$\Delta \mathbf{P}_{\text{cyc}} = \oint_0^1 d\lambda \frac{d\mathbf{P}}{d\lambda} \quad (\text{cyclic evolution: } H_{\lambda=0} = H_{\lambda=1}). \quad (36)$$

From (31), it follows that $\Delta \mathbf{P}_{\text{cyc}}$ is either exactly zero or else exactly $e\mathbf{R}/\Omega$ for some non-zero lattice vector \mathbf{R} . The latter case corresponds to the “quantized charge transport” (or “quantum pumping”) first discussed by *Thouless* [24].

Now suppose we follow the locations of the Wannier centers \mathbf{r}_n during this adiabatic evolution. Since the initial and final points are the same, the Wannier centers must return to their initial locations at the end of the cyclic evolution. However, they can do so in two ways, as illustrated in Figs. 10a,b. If each Wannier center returns to itself, then $\Delta \mathbf{P}_{\text{cyc}}$ is truly zero. However, as illustrated in Fig. 10b, this need not be the case; it is only necessary that each Wannier center return to one of its periodic images. If it does not return to itself, a quantized charge transport occurs.⁸

4 Implications for Ferroelectrics

Most of the fundamental and technological interest in FE materials arises from their polarization and related properties, including the dielectric and piezoelectric responses. The rigorous formulation of the polarization has allowed detailed quantitative investigation of these properties from first prin-

⁸ We emphasize that this discussion is highly theoretical. While such a situation could occur in principle, it is not known to occur in practice in any real ferroelectric material.

principles. In this section, we give an overview of the analysis of three key quantities – the spontaneous polarization, the Born effective charges, and the piezoelectric response – and discuss case studies for specific perovskite oxides, primarily the tetragonal phase of the FE perovskite oxide KNbO_3 .

4.1 Spontaneous Polarization

The experimental P_s values for the most common single-crystal FE perovskites in their different crystalline phases have been known for several decades. However, despite the fact that P_s is the very property characterizing FE materials, there was no theoretical access to it until 1993. As discussed above, the common-wisdom microscopic definition of what P_s was basically incorrect. The modern theory of polarization provides the correct definition of P_s , as well as the theoretical framework allowing one to compute it from the occupied Bloch eigenstates of the self-consistent crystalline Hamiltonian. As soon as *King-Smith* and *Vanderbilt* developed the theory [18] – as outlined in Sect. 3 – *Resta* et al. [25] implemented and applied it to compute the spontaneous polarization of a prototypical perovskite oxide from first principles.

The case study was KNbO_3 in its tetragonal phase, in a frozen-nuclei geometry taken from crystallographic data. The reciprocal cell is tetragonal: the integral in (19) was computed according to Sect. 3.2 (see Fig. 7), using the occupied Kohn–Sham orbitals [5]. The electronic phase so evaluated depends on the choice of the origin in the crystalline cell, but translational invariance is restored when the nuclear contribution is accounted for.

The computed phase turns out to be approximately $\pi/3$. This is large enough that it is advisable to check whether the correct choice of branch has been made for the multivalued function “ $\Im \ln$ ” in (22), in order to eliminate the 2π ambiguity discussed in Sect. 3.3. This is done by repeating the calculation for smaller amplitudes of the FE distortion and making sure that the phase is a continuous function of the amplitude, as discussed earlier at the end of Sect. 3.3.

The first-principles calculation of [25] for tetragonal KNbO_3 yielded a value $P_s = 0.35 \text{ C/m}^2$, to be compared to a best experimental value of 0.37 C/m^2 . A similar level of agreement was later found for other perovskites and using computational packages with different technical ingredients.

One aspect of the calculation deserves some comment. As stated above, we have adopted a frozen-nuclei approach, which in principle is appropriate for describing the polarization of the zero-temperature structure only. In the calculation for KNbO_3 discussed above, as well as in other calculations in the literature, one addresses instead the spontaneous polarization of a finite-temperature crystalline phase. In fact, the tetragonal phase of KNbO_3 only exists between 225 and 418 °C, while the equilibrium structure at zero temperature is rhombohedral and *not* tetrahedral. Crystallographic data provide

the time-averaged crystalline structure, while polarization-reversal experiments provide the time-averaged spontaneous polarization. The question is then whether the time-averaged polarization is equal, to a good approximation, to the polarization of the time-averaged structure, as the latter is in fact the quantity that is actually computed. The answer to this question is essentially “yes”, supported by the finding that the macroscopic polarization is roughly linear, at the $\pm 10\text{--}20\%$ level, in the amplitude of the structural distortion. This essential linearity could *not* have been guessed from model arguments, and in fact has only been discovered from the ab-initio calculations [25, 26].

4.2 Anomalous Dynamical Charges

The Born effective-charge tensors measure the coupling of a macroscopic field $\boldsymbol{\mathcal{E}}$ with relative sublattice displacements (zone-center phonons) in the crystal; they also go under the name of dynamical charges or infrared charges. Within an extreme rigid-ion model the Born charge coincides with the static charge of the model ion (“nominal” value), while in a real material the Born charges account for electronic polarization as well. Before the advent of the modern theory of polarization in the 1990s, the relevance of dynamical charges to the phenomenon of ferroelectricity had largely been overlooked.

There are two equivalent definitions of the Born tensor Z_s^* . 1. $Z_{s,\alpha\beta}^*$, as defined in (9), measures the change in polarization \mathbf{P} in the α direction linearly induced by a sublattice displacement \mathbf{u}_s in the β direction in zero macroscopic electric field. (Other kinds of effective charge can be defined using other electrical boundary conditions [27], but this choice of $\boldsymbol{\mathcal{E}} = 0$ is the “Born charge” one.) 2. Alternatively, $Z_{s,\alpha\beta}^*$ measures the force \mathbf{F} linearly induced in the α direction on the s th nucleus by a uniform macroscopic electric field $\boldsymbol{\mathcal{E}}$ in the β direction (at zero displacement):

$$F_{s,\alpha} = -e \sum_{\beta} Z_{s,\beta\alpha}^* \mathcal{E}_{\beta}. \quad (37)$$

Notice that, in low-symmetry situations, Z_s^* is not symmetric in its Cartesian indices. Since any rigid translation of the whole solid does not induce macroscopic polarization, the Born effective-charge tensors obey

$$\sum_s Z_{s,\alpha\beta}^* = 0, \quad (38)$$

a result that is generally known as the “acoustic sum rule” [28].

The Berry-phase theory of polarization naturally leads to an evaluation of the derivative in (9) as a finite difference, and this is the way most Z_s^* calculations are performed for FE perovskites. However, expressions (9) or (37) based on linear response approaches [20] can be used

whenever an electronic-structure code implementing such an approach (e.g., <http://www.abinit.org/>, <http://www.pwscf.org>) is available.

The Born effective-charge tensors are a staple quantity in the theory of lattice dynamics for polar crystals [29], and their experimental values have long been known to a very good accuracy for simple materials such as binary ionic crystals and simple semiconductors. As for FE materials, some experimentally derived values for BaTiO₃ were proposed long ago [30]. However, the subject remained basically neglected until 1993, when [25] appeared. This ab-initio calculation demonstrated that in FE perovskites the Born charges are strongly “anomalous”, and that this anomaly has much to do with the phenomenon of ferroelectricity. Since then, ab-initio investigations of the Z_s^* have become a standard tool for the study of FE oxides, and have provided invaluable insight into ferroelectric phenomena [4, 27, 31].

For most FE ABO₃ perovskites the nominal static charges are either 1 or 2 for the A cation, either 5 or 4 for the B cation, and -2 for oxygen. On the contrary, modern calculations have demonstrated that in these materials the Born charges typically assume much larger values. We discuss this feature using as a paradigmatic example the case of KNbO₃, which was the first to be investigated in 1993 [25]. The paraelectric prototype structure is cubic, and the cations sit at cubic sites, thus warranting isotropic Z_s^* tensors. The oxygens sit instead at noncubic sites so that Z_O^* has two independent components: one (called O1) for displacements pointing towards the Nb ion, and the other (called O2) for displacements in the orthogonal plane. The results of [25] are that Z_s^* takes values of 0.8 for K, 9.1 for Nb, -6.6 for O1, and -1.7 for O2. Both the Nb and O1 values are thus strongly anomalous, being much larger (in modulus) than the corresponding nominal values.

Such a finding appears counterintuitive, since one would expect that the extreme ionic picture provides an upper bound on the ionic charges. In partly covalent oxides one would naively guess values smaller, and *not* larger, than the nominal ones, for all ions. Instead, anomalous values for the transition element and for O1 ions have been later confirmed by all subsequent calculations, using quite different technical ingredients and/or for other perovskite oxides [27, 32, 33]. The physical origin of the giant dynamical charges is precisely the borderline ionic-covalent character of ABO₃ oxides, specifically owing to the hybridization of $2p$ oxygen orbitals with the $4d$ or $5d$ orbitals of the B cation. A thorough discussion of this issue can be found in [4, 31].

4.3 Piezoelectric Properties

Piezoelectricity has been an intriguing problem for many years. Even the *formal* proof that piezoelectricity is a well-defined bulk property – independent of surface termination – is relatively recent (1972), and is due to R. M. Martin. This proof was challenged, and the debate lasted for two decades [10–16]. The piezoelectric tensor γ measures the coupling of a macroscopic field \mathcal{E}

with macroscopic strain. The root of the problems with understanding piezoelectricity is in the fact that – within periodic Born–von Kármán boundary conditions – strain is *not* a perturbing term in the Hamiltonian; instead, it amounts to a change of boundary conditions.

As in the case of the Born effective charges, there are two equivalent definitions of γ , which is a third-rank Cartesian tensor. 1. $\gamma_{\delta\alpha\beta}$ measures the polarization linearly induced in the δ direction by macroscopic strain $\epsilon_{\alpha\beta}$ at zero field:

$$\gamma_{\delta\alpha\beta} = \frac{\partial P_\delta}{\partial \epsilon_{\alpha\beta}}. \quad (39)$$

2. Alternatively, $\gamma_{\delta\alpha\beta}$ measures the stress $\sigma_{\alpha\beta}$ linearly induced by a macroscopic field in the δ direction at zero strain:

$$\sigma_{\alpha\beta} = \sum_\delta \gamma_{\delta\alpha\beta} E_\delta. \quad (40)$$

The first ab-initio calculation of piezoelectric constants appeared in 1989 [34]; therein, the III–V semiconductors were chosen as case studies. This work exploited (40), linear-response theory [20], and the Nielsen–Martin stress theorem [35–37]. Nowadays, most calculations of the piezoelectric effect in FE materials are based on the finite-difference approximation to (39), in conjunction with a Berry-phase calculation. The first such calculation, for PbTiO_3 , was performed in 1998 [38, 39]; other calculations for other materials, including some ordered models of FE alloys, were performed soon afterwards [40, 41].

Macroscopic strain typically induces *internal strain* as well. That is, when the cell parameters are varied, the internal coordinates relax to new equilibrium positions, in general not mandated by symmetry. This effect is characterized by a set of material-dependent constants known as internal-strain parameters. In principle, there is no need to deal with internal strain separately; (39) is in fact exact, *provided that* the internal coordinates are continually relaxed to their equilibrium values as the strain is applied. However, it is often more convenient to exploit linearity and to compute the piezoelectric tensor γ as the sum of two separate terms. The first term is the “clamped-nuclei” one, evaluated by applying a homogeneous macroscopic strain without including internal strain (i.e., without allowing any internal coordinates to relax). The second term accounts only for the change in polarization induced by the internal strain, and can easily be evaluated – knowing the internal-strain parameters and the Born charges – as the change in polarization associated with induced displacements associated with polar zone-center phonons.

Whenever the crystal has a nonvanishing spontaneous polarization, the definition of the piezoelectric response becomes more subtle. The simplest and most natural definition, usually called the “proper” piezoelectric response [42], is based on the current density flowing through the bulk of a

sample in adiabatic response to a slow strain deformation, as in Fig. 3b. The proper response corresponds in most circumstances to the actual experimental setup, and, furthermore, is the one having the most direct link to the modern theory. In order to evaluate a proper piezoelectric coefficient as a finite difference, it is enough to adopt a Berry-phase formulation in scaled coordinates as in (26) and evaluate derivatives of the $\varphi_{n,j}$ [19, 42]. It is worth emphasizing that the arbitrary quantum of polarization, Sect. 3.3, does *not* give rise to any ambiguity in the proper piezoelectric response, since its strain derivative is zero [42].

5 Further Theoretical Developments

In this section, we briefly introduce a few advanced topics associated with the theory of polarization, providing references to the literature for those readers who desire a fuller treatment.

5.1 Polarization in an Applied Electric Field

Up to this point, our treatment has been limited to the case of insulators in a vanishing macroscopic electric field. Clearly there are many situations, in which it is very desirable to treat the application of an electric field directly, especially for FEs and for other types of dielectric materials. However, the usual theory of electron states in crystals is based on Bloch's theorem, which requires that the crystal potential be periodic. This rules out the presence of a macroscopic electric field \mathcal{E} , since this would imply a change by $e\mathcal{E} \cdot \mathbf{R}$ of the electron potential under a translation by a lattice vector \mathbf{R} .

Indeed, the difficulties in treating the case of a finite electric field are quite severe. Even a small field changes the qualitative nature of the energy eigenstates drastically, and a theory based on such energy eigenstates is no longer useful. Even more seriously, because the potential is unbounded from below, there is no well-defined ground state of the electron system! The “state” that one has in mind is one in which all “valence” states are occupied and all “conduction” states are empty. However, for an insulator of gap E_g in a field \mathcal{E} , it is always possible to lower the energy of the system by transferring electrons from the valence band in one region to the conduction band in a region a distance $\gg L_t = E_g/\mathcal{E}$ down-field. This “Zener tunneling” is analogous to the autoionization that also occurs, in principle, for an atom or molecule in a finite electric field.

Nevertheless, we expect that if we start with an insulating crystal in its ground state and adiabatically apply a modest electric field, there should be a reasonably well-defined “state” that we can solve for. Indeed, perturbative treatments of the application of an electric field have long been known, and are a standard feature of modern electronic structure theory (for a review,

see [20]). In 1994, *Nunes* and *Vanderbilt* [43] proposed a Wannier-function-based solution to the finite-field problem that, while successful in principle, was not very useful in practice. Transforming back to Bloch functions, *Nunes* and *Gonze* showed in 2001 [44] how the known perturbative treatments could be obtained (and, in some cases, extended) by deriving them from a variational principle based on minimizing an energy functional F of the form

$$F = E_{\text{KS}}(\{\psi_{n\mathbf{k}}\}) - \mathcal{E} \cdot \mathbf{P}(\{\psi_{n\mathbf{k}}\}). \quad (41)$$

Here, $E_{\text{KS}}(\{\psi_{n\mathbf{k}}\})$ is the usual Kohn–Sham energy per unit volume expressed as a function of all occupied Bloch functions, and similarly $\mathbf{P}(\{\psi_{n\mathbf{k}}\})$ is the usual zero-field Berry-phase expression for the electronic polarization. This equation is to be minimized with respect to all $\{\psi_{n\mathbf{k}}\}$ in the presence of a given field \mathcal{E} ; thus, the Bloch functions at minimum become functions of \mathcal{E} , so that the first term in (41) also acquires an implicit \mathcal{E} dependence.

Subsequently, *Souza* et al. [45] and *Umari* and *Pasquarello* [46] demonstrated that (41) was suitable for use as an energy functional for a variational approach to the *finite*-field problem as well. The justification for such a procedure is not obvious, in view of the fact that the occupied wavefunction solutions $\{\psi_{n\mathbf{k}}\}$ are *not eigenstates* of the Hamiltonian. Instead, they can be regarded as providing a representation of the one-particle density matrix, which can be shown to remain periodic in the presence of a field [45, 47], or by treating the system from a time-dependent framework [47] in which the field is slowly turned on from zero.

Because the “state” of interest is, in principle, only a long-lived resonance in the presence of a field, there should be some sense in which the above theory fails to produce a perfectly well-defined solution. This is so, and it comes about in an unfamiliar way: the variational solution breaks down if the k -point sampling is taken to be too fine. Indeed, if $\Delta k \ll 1/L_t$, where $L_t = E_g/\mathcal{E}$ is the Zener tunneling length mentioned above, the variational procedure fails [45, 46]. The theory is thus limited to modest fields (more precisely, to $\mathcal{E} \ll E_g/a$, where a is a lattice constant).

In any case, it is interesting to discover that the problem of computing \mathbf{P} in an electric field provides, in a sense, the solution to the problem of computing *any* property of an insulator in a finite field: it is precisely the introduction of the Berry-phase polarization into (41) that solves the problem.

5.2 Interface Theorem and the Definition of Bound Charge

It is well known from elementary electrostatics that the bound charge density in the presence of a spatially varying polarization field is

$$\rho_b(\mathbf{r}) = -\nabla \cdot \mathbf{P}(\mathbf{r}), \quad (42)$$

where $\rho_b(\mathbf{r})$ and $\mathbf{P}(\mathbf{r})$ are macroscopic fields (i.e., coarse grained over a length scale much larger than a lattice constant). As long as the polarization changes

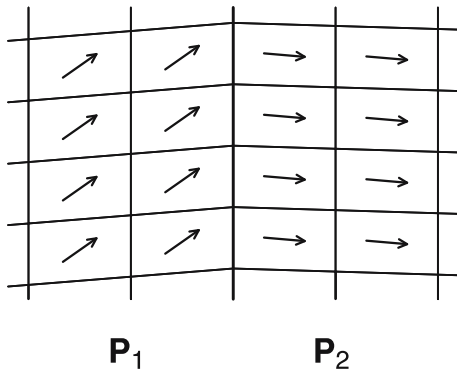


Fig. 11. Sketch of epitaxial interface between two different FE crystals, or between FE domains of a single crystal. The difference in the interface-normal components of \mathbf{P}_1 and \mathbf{P}_2 leads to an interface bound charge given by (43)

gradually over space, as in response to a gradual strain field or composition gradient, there is no difficulty in associating $\mathbf{P}(\mathbf{r})$ with the Berry-phase polarization of Sect. 3.3 computed for a crystal whose global structure matches the local structure at \mathbf{r} . There is no difficulty with respect to the “choice of branch” (see Sect. 3.3) since the gradual variation of \mathbf{P} allows the choice of branch to be followed from one region to another, and the bound charge of (42) is clearly independent of branch.

The case of an interface between two FE materials, or of a FE domain wall in a single FE material, is more interesting. Consider an epitaxial interface between two FE materials, as shown in Fig. 11. One naively expects a relation of the form $\sigma_b = \hat{\mathbf{n}} \cdot (\mathbf{P}_1 - \mathbf{P}_2)$, where σ_b is the macroscopic bound surface charge at the interface and $\hat{\mathbf{n}}$ is a unit vector normal to the interface. However, in general the two materials may be quite dissimilar, so that a choice of branch needs to be made for the Berry-phase expressions for \mathbf{P}_1 and \mathbf{P}_2 separately, leading to an uncertainty in the definition of the bound interface charge σ_b .

Indeed, a careful analysis of situations of this type is given in [23], where it is shown that the interface bound charge is given by

$$\sigma_b = \hat{\mathbf{n}} \cdot (\mathbf{P}_1 - \mathbf{P}_2) \quad \text{mod} \quad \frac{e}{A_{\text{int}}} \quad (43)$$

under the following conditions: 1. the epitaxial match is perfect and dislocation free, with a common 1×1 interface unit cell area A_{int} ; and 2. material 1, material 2, and the interface are all insulating, with a common gap. The interface need not be as abrupt as illustrated in Fig. 11; some relaxations may occur in the first few neighboring cells to the interface. It is only necessary to identify \mathbf{P}_1 and \mathbf{P}_2 with the Berry-phase polarizations of the crystalline structures far enough from the interface for these relaxations to have healed, and to interpret σ_b as the macroscopic excess interface charge density integrated over this interface region.

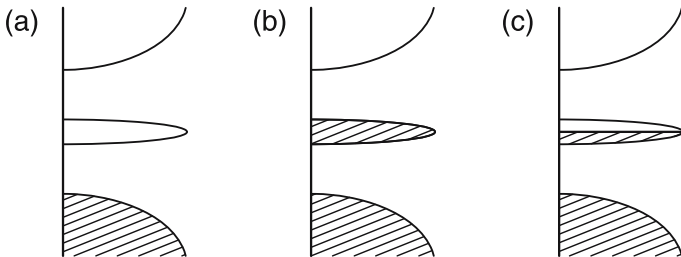


Fig. 12. Sketch of density of states that could be associated with the epitaxial interface of Fig. 11. Valence bands of materials 1 and 2 are hashed; conduction bands are unfilled; and a band of interface states may either be (a) entirely empty; (b) entirely filled; or (c) partially filled (i.e., metallic)

The appearance of the caveat “mod e/A_{int} ” in (43) is remarkable, and confirms that, at least in principle, there can be an uncertainty in the definition of the interface bound charge. This can be understood in two ways. First, the uncertainty of \mathbf{P}_1 and \mathbf{P}_2 mod $e\mathbf{R}/\Omega$ leads to the uncertainty $(e\mathbf{R}/\Omega) \cdot \hat{\mathbf{n}} = e/A_{\text{int}}$, as can be confirmed from simple geometry. Second, on more physical grounds, we can expect such an uncertainty because of the flexibility of the condition (2) stating that material 1, material 2, and the interface must all be insulating with a common gap. Consider a situation like that illustrated in Fig. 12, where there are m (counting spin) discrete interface bands lying near the middle of a gap that is common to both materials 1 and 2. Panels (a) and (b) both show situations that satisfy the conditions (1) and (2) of (43), but the interface charge clearly differs by precisely em/A_{int} between these two situations. Panel (c) shows a situation that does not satisfy the stated conditions, as the interface is metallic. In this case, the charge counting may be done either with reference to the situation of Panel (a), in which case one either says that a large free-electron charge density is present on top of the bound charge defined by situation (a), or else that a large free-hole charge density is present on top of the bound charge defined by situation (b).

Similar considerations lead to a “surface theorem” [23] relating the macroscopic bound surface charge at a FE/vacuum interface to the surface-normal component of the polarization of the underlying medium, mod e/A_{surf} .

In practice, the change in polarization ($\mathbf{P}_1 - \mathbf{P}_2$) between two FE materials is usually much smaller than the quantum, in which case there is a “natural” choice of branch for the definition of the interface bound charge σ_{int} in (43). However, for materials with large polarizations, such as certain Pb- and Bi-based perovskites (see, e.g., [48]), the ambiguity in the definition of interface bound charge may need to be considered with care.

5.3 Many-Body and Noncrystalline Generalizations

The treatment given so far is based on the 1993 paper by *King-Smith* and *Vanderbilt* [18] and assumes an independent-particle scheme, where polarization is evaluated as a Berry phase of one-electron orbitals, typically the Kohn–Sham ones [5], which in a crystalline material assume the Bloch form. Shortly after the appearance of [18], *Ortiz* and *Martin* [49] provided the many-body generalization of the theory, where polarization is expressed as a Berry phase of the many-body wavefunction.

A subsequent development, by *Resta* [50], provides a unified treatment of macroscopic polarization, dealing on the same footing with either independent-electron or correlated systems, and with either crystalline or disordered systems. This approach is based on a novel viewpoint, which goes under the (apparently oxymoronic) name of “single-point Berry phase”. On practical grounds, such a single-point Berry phase is universally adopted in order to evaluate macroscopic polarization within first-principle simulations of disordered systems.⁹

Here, we give a flavor of the approach, while we refer to the literature for more complete accounts [50–52]. Let us consider, for the sake of simplicity, a system of N one-dimensional spinless electrons. The many-body ground wavefunction is then $\Psi(x_1, x_2, \dots, x_j, \dots, x_N)$, and all the electrons are confined to a segment of length L . Eventually, we will be interested in the thermodynamic limit, defined as the limit $N \rightarrow \infty$ and $L \rightarrow \infty$, while the density N/L is kept constant. The wavefunction Ψ is Born–von Kàrmàn periodic, with period L , over each electronic variable x_j separately. Equivalently, one can imagine the electrons to be confined in a circular rail of length L : the coordinates x_j are then proportional to the angles $2\pi x_j/L$, defined mod 2π .

The key quantity is the ground-state expectation value

$$z_N = \langle \Psi | U | \Psi \rangle = \int_0^L dx_1 \dots \int_0^L dx_N |\Psi(x_1, \dots, x_N)|^2 U(x_1, \dots, x_N), \quad (44)$$

where the unitary operator U , called a “twist operator”, is defined as

$$U(x_1, \dots, x_N) = \exp\left(i \frac{2\pi}{L} \sum_{j=1}^N x_j\right), \quad (45)$$

and clearly is periodic with period L . The expectation value z_N is a dimensionless complex number, whose modulus is no larger than one. The electronic contribution to the macroscopic polarization of the system can be expressed in the very compact form [50, 52]:

$$P_{\text{el}} = -\frac{e}{2\pi} \lim_{N \rightarrow \infty} \Im \ln z_N, \quad (46)$$

⁹ <http://www.cpmid.org/>

Notice that, for a one-dimensional system, the polarization has the dimensions of a charge (dipole per unit length). The essential ingredient in (46) is $\Im \ln z_N$, i.e., the *phase* of the complex number z_N . This phase can be regarded as a very peculiar kind of Berry phase.

So far, we have assumed neither independent electrons nor crystalline order; (46) is in fact a very general definition of macroscopic polarization. In the special case of a crystalline system of independent electrons, the many-body wavefunction Ψ is a Slater determinant of single-particle orbitals. For any finite N , (44) and (46) can then be shown to be equivalent to a discretized Berry phase of the occupied bands, of the same kind as those addressed in Sect. 3.2.

5.4 Polarization in Kohn–Sham Density-Functional Theory

Suppose we are given the ground-state interacting electron density $n(\mathbf{r})$ of an insulating crystal. From this, the Kohn–Sham theory [5] gives a unique prescription for determining a noninteracting system, with an effective Kohn–Sham potential, having the same ground-state electron density. The following question then arises: If one computes the Berry-phase polarization from this noninteracting Kohn–Sham system, does one arrive, in principle, at the correct many-body polarization?

As shown by *Gonze et al.* [53, 54], the answer to this question is that, in general, one *does not* obtain the correct polarization.

There are three ways to approach this issue. First, one may restrict one’s considerations to a strictly infinite crystalline system with a given cell shape and with a uniform macroscopic electric field \mathcal{E} [53, 54]. One can then demonstrate a generalized Hohenberg–Kohn theorem stating that a given periodic density $n(\mathbf{r})$ and macroscopic polarization \mathbf{P} together uniquely determine a periodic external potential $V_{\text{per}}(\mathbf{r})$ and electric field \mathcal{E} . Moreover, the corresponding Kohn–Sham construction involves finding an effective periodic potential $V_{\text{per}}^{\text{KS}}(\mathbf{r})$ and effective electric field \mathcal{E}^{KS} that yield, for a *noninteracting* system, the same $n(\mathbf{r})$ and \mathbf{P} . In this theory of *Gonze et al.* [53, 54], the polarization is correct by construction, but at the expense of introducing a correction $\mathcal{E}^{\text{KS}} - \mathcal{E}$ that they referred to as an “exchange-correlation electric field”. The reader is directed to [53, 54] for details.

A second approach is to consider conventional Kohn–Sham theory in the context of finite macroscopic sample geometries, surrounded by vacuum, and having particular surfaces, interfaces, or FE domain configurations. An analysis of this type [55] again leads to the conclusion that the local polarization obtained from exact Kohn–Sham theory is not, in general, the correct one. In general, one finds that the *longitudinal* part of the polarization field $\mathbf{P}(\mathbf{r})$ must be correct (since the corresponding charge density $-\nabla \cdot \mathbf{P}$ must be correct), but the *transverse* part of the polarization field need *not* be correct.

A third approach is suggested by (44). The wavefunction Ψ_{KS} of the noninteracting Kohn–Sham system is a Slater determinant and is necessarily

different from Ψ , despite sharing the same single-particle density. Since the twist operator U is a genuine many-body operator, its expectation value over Ψ_{KS} is in general different from the one over Ψ . The polarization (46), is different as well.

5.5 Localization, Polarization, and Fluctuations

An insulator is distinguished from a metal by its vanishing dc conductivity at low temperature. In contrast to what happens in metals, the electronic charge in insulators (and quite generally nonmetals) cannot flow freely under an applied dc field; instead it undergoes static polarization. As first pointed out in 1964 by *Kohn*, this fact stems from a basic qualitative difference in the organization of the electrons in their *ground state* [56]. The modern theory of polarization has provided much insight into such different organization.

An insulator sustains a nontrivial, material-dependent, macroscopic polarization, which is nonvanishing whenever the Hamiltonian is noncentrosymmetric. Instead, the polarization of a metallic sample is determined by the Faraday-cage effect and therefore is *not* a well-defined property of the bulk material. At the independent-electron level, the polarization of a crystalline insulator can be expressed in terms of Wannier functions, as discussed in Sect. 3.5. The key feature is that, in insulators, a set of well-localized orbitals (the Wannier functions) spans the same Hilbert space as do the Bloch orbitals of the occupied bands. This is indeed a qualitative difference in the organization of the electrons between insulators and metals. In the latter, in fact, it is impossible to span the Hilbert space of the occupied Bloch orbitals using well-localized orbitals. This statement can be made more precise by addressing the spherical second moments of the charge distributions of the localized orbitals [57]. Such second moments can be made finite in insulators, while they necessarily diverge in metals, as discussed below. It therefore emerges that the key qualitative feature differentiating the ground state of an insulator from that of a metal is electron localization. This applies well beyond the independent-electron level; in fact, as emphasized already by *Kohn* in 1964, the ground wavefunction of *any* insulator is localized. The modern theory of polarization leads to a simple and elegant measure of such localization [52].

It is expedient to refer, as in Sect. 5.3, to a system of N one-dimensional spinless electrons. From (46) it is clear that macroscopic polarization is a well-defined quantity whenever the modulus of z_N is nonvanishing in the large N limit. In the latter case, the second moment of the electron distribution can be defined, following *Resta* and *Sorella* [58], as

$$\langle x^2 \rangle_{\text{c}} = - \lim_{N \rightarrow \infty} \frac{1}{N} \left(\frac{L}{2\pi} \right)^2 \ln |z_N|^2, \quad (47)$$

where the subscript “c” stands for “cumulant”. The same concept generalizes to a Cartesian tensor $\langle r_\alpha r_\beta \rangle_{\text{c}}$ in three dimensions. This localization tensor,

having the dimension of a squared length, is an intensive property and applies on the same footing to ordered/disordered and correlated/uncorrelated many-electron systems; it is finite in any insulator and divergent in any metal. In the special case of an insulating crystalline system of independent electrons, the meaning of $\langle r_\alpha r_\beta \rangle_c$ becomes more perspicuous. In fact, the trace of this tensor is a lower bound to the average spherical second moment of the charge distributions of the Wannier functions of the occupied bands [57]; in the metallic case, the lower bound is formally divergent.

Two important questions were left unanswered by Resta and Sorella. Given that in any insulator the localization tensor $\langle r_\alpha r_\beta \rangle_c$ is, at least in principle, a well-defined ground-state observable, the first question is whether this can be measured, and by which kind of experiments. The second question is whether $\langle r_\alpha r_\beta \rangle_c$ can be related in some way to dc conductivity, given that the vanishing of the latter characterizes – in addition to macroscopic polarization – the insulating state of matter. Both questions received a positive answer owing to the work of Souza et al. [51]. They began by showing that $\langle r_\alpha r_\beta \rangle_c$ measures the mean-square fluctuation of the polarization; then, by exploiting a fluctuation-dissipation theorem, they explicitly linked $\langle r_\alpha r_\beta \rangle_c$ to the conductivity of the system.

6 Summary

In this chapter we have reviewed the physical basis of the modern theory of polarization. From a physical viewpoint, we have emphasized that the polarization may be defined in terms of the accumulated adiabatic flow of current occurring as a crystal is modified or deformed, and have discussed the consequences of this picture for the theory of polarization reversal and piezoelectric effects in FE materials. From a mathematical viewpoint, we have explained how the polarization is closely related to a Berry phase of the Bloch wavefunctions as the wavevector traverses the Brillouin zone, and to the centers of charge of the Wannier functions that may be constructed from the Bloch wavefunctions. An essential feature of the theory is the fact that the polarization is formally defined only modulo a “quantum of polarization,” or equivalently, that it must be regarded as a multivalued quantity. We have also attempted to clarify how piezoelectric effects and surface and interface charges are to be understood in terms of the modern theory.

The capability of computing polarization is now available in almost all commonly used software packages for bulk electronic-structure calculations. While initially formulated in vanishing electric field, the case of finite field can be treated by letting the external electric field couple to the polarization while retaining the Bloch form of the wavefunctions. These methods allow for the computation of numerous quantities of interest, including spontaneous polarization, Born effective charges, linear piezoelectric coefficients, nonlinear dielectric and piezoelectric responses, and the like. Indeed, taken together, they provide a robust and powerful foundation for modern computational studies of the polarization-related properties of FE materials.

References

- [1] L. D. Landau, E. M. Lifshitz: *Electrodynamics of Continuous Media* (Pergamon, Oxford 1984) [31](#)
- [2] O. F. Mossotti: Azioni e deformazioni nei dielettrici, *Memorie di Matematica e di Fisica della Società Italiana delle Scienze Residente in Modena* **24**, 49 (1850) [31](#)
- [3] R. Clausius: *Die Mechanische Behandlung der Electrica* (Vieweg, Berlin 1879) [31](#)
- [4] M. Posternak, R. Resta, A. Baldereschi: Role of covalent bonding in the polarization of perovskite oxides: The case of KNbO_3 , *Phys. Rev. B* **50**, 8911 (1994) [33](#), [55](#)
- [5] S. Lundqvist, N. H. March (Eds.): *Theory of the Inhomogeneous Electron Gas* (Plenum, New York 1983) [33](#), [42](#), [53](#), [61](#), [62](#)
- [6] W. E. Pickett: Pseudopotential methods in condensed matter applications, *Comput. Phys. Rep.* **9**, 115 (1989) [33](#)
- [7] C. Kittel: *Introduction to Solid State Physics*, 7th ed. (Wiley, New York 1996) [33](#), [35](#), [38](#), [42](#)
- [8] N. W. Ashcroft, N. D. Mermin: *Solid State Physics* (Saunders, Philadelphia 1976) [33](#), [35](#), [38](#), [42](#)
- [9] R. M. Martin: Comment on calculations of electric polarization in crystals, *Phys. Rev. B* **9**, 1998 (1974) [35](#)
- [10] R. M. Martin: Piezoelectricity, *Phys. Rev. B* **5**, 1607 (1972) [36](#), [55](#)
- [11] R. M. Martin: Comment on piezoelectricity under hydrostatic pressure, *Phys. Rev. B* **6**, 4874 (1972) [36](#), [55](#)
- [12] W. F. Woo, W. Landauer: Comment on “piezoelectricity under hydrostatic pressure”, *Phys. Rev. B* **6**, 4876 (1972) [36](#), [55](#)
- [13] R. Landauer: Pyroelectricity and piezoelectricity are not true volume effects, *Solid State Commun.* **40**, 971 (1981) [36](#), [55](#)
- [14] C. Kallin, B. J. Halperin: Surface-induced charge disturbances and piezoelectricity in insulating crystals, *Phys. Rev. B* **29**, 2175 (1984) [36](#), [55](#)
- [15] R. Landauer: Introduction to ferroelectric surfaces, *Ferroelectrics* **73**, 41 (1987) [36](#), [55](#)
- [16] A. K. Tagantsev: Electric polarization in crystals and its response to thermal and elastic perturbations, *Phase Transitions* **35**, 119 (1991) [36](#), [55](#)
- [17] R. Resta: Theory of the electric polarization in crystals, *Ferroelectrics* **136**, 51 (1992) [38](#), [40](#), [41](#)
- [18] R. D. King-Smith, D. Vanderbilt: Theory of polarization of crystalline solids, *Phys. Rev. B* **47**, 1651 (1993) [38](#), [41](#), [42](#), [46](#), [53](#), [61](#)
- [19] R. Resta: Macroscopic polarization in crystalline dielectrics: The geometric phase approach, *Rev. Mod. Phys.* **66**, 899 (1994) [38](#), [41](#), [42](#), [46](#), [57](#)
- [20] S. Baroni, S. de Gironcoli, A. Dal Corso, P. Giannozzi: Phonons and related crystal properties from density-functional perturbation theory, *Rev. Mod. Phys.* **73**, 515 (2001) [41](#), [54](#), [56](#), [58](#)
- [21] A. Shapere, F. Wilczek (Eds.): *Geometric Phases in Physics* (World Scientific, Singapore 1989) [42](#), [43](#)
- [22] R. Resta: Manifestations of Berry’s phase in molecules and condensed matter, *J. Phys. Condens. Matter* **12**, R107 (2000) [42](#), [43](#)

- [23] D. Vanderbilt, R. D. King-Smith: Electric polarization as a bulk quantity and its relation to surface charge, *Phys. Rev. B* **48**, 4442 (1993) [42](#), [59](#), [60](#)
- [24] D. J. Thouless: Quantization of particle transport, *Phys. Rev. B* **27**, 6083 (1983) [52](#)
- [25] R. Resta, M. Posternak, A. Baldereschi: Towards a quantum theory of polarization in ferroelectrics: The case of KNbO_3 , *Phys. Rev. Lett.* **70**, 1010 (1993) [53](#), [54](#), [55](#)
- [26] S. Dall’Olio, R. Dovesi, R. Resta: Spontaneous polarization as a Berry phase of the Hartree-Fock wave function: The case of KNbO_3 , *Phys. Rev. B* **56**, 10105 (1997) [54](#)
- [27] P. Ghosez, J.-P. Michenaud, X. Gonze: Dynamical atomic charges: The case of ABO_3 compounds, *Phys. Rev. B* **58**, 6224 (1998) [54](#), [55](#)
- [28] R. Pick, M. H. Cohen, R. M. Martin: Microscopic theory of force constants in the adiabatic approximation, *Phys. Rev. B* **1**, 910 (1970) [54](#)
- [29] M. Born, K. Huang: *Dynamical Theory of Crystal Lattices* (Oxford University Press, Oxford 1954) [55](#)
- [30] J. D. Axe: Apparent ionic charges and vibrational eigenmodes of BaTiO_3 and other perovskites, *Phys. Rev.* **157**, 429 (1967) [55](#)
- [31] R. Resta: Dynamical charges in oxides: Recent advances, *J. Phys. Chem. Solids* **61**, 153 (1999) [55](#)
- [32] W. Zhong, R. D. King-Smith, D. Vanderbilt: Giant LO-TO splittings in perovskite ferroelectrics, *Phys. Rev. Lett.* **72**, 3618 (1994) [55](#)
- [33] P. Ghosez, X. Gonze, P. Lambin, J.-P. Michenaud: Born effective charges of barium titanate: Band-by-band decomposition and sensitivity to structural features, *Phys. Rev. B* **51**, 6765 (1995) [55](#)
- [34] S. de Gironcoli, S. Baroni, R. Resta: Piezoelectric properties of III-V semiconductors from first-principles linear-response theory, *Phys. Rev. Lett.* **62**, 2853 (1989) [56](#)
- [35] O. H. Nielsen, R. M. Martin: First-principles calculation of stress, *Phys. Rev. Lett.* **50**, 697 (1983) [56](#)
- [36] O. H. Nielsen, R. M. Martin: Quantum-mechanical theory of stress and force, *Phys. Rev. B* **32**, 3780 (1985) [56](#)
- [37] O. H. Nielsen, R. M. Martin: Stresses in semiconductors: Ab initio calculations on Si, Ge, and GaAs, *Phys. Rev. B* **32**, 3792 (1985) [56](#)
- [38] G. Sági-Szabó, R. E. Cohen, H. Krakauer: First-principles study of piezoelectricity in PbTiO_3 , *Phys. Rev. Lett.* **80**, 4321 (1998) [56](#)
- [39] H. Fu, R. E. Cohen: Polarization rotation mechanism for ultrahigh electromechanical response in single-crystal piezoelectrics, *Nature* **403**, 281 (2000) [56](#)
- [40] G. Sági-Szabó, R. E. Cohen, H. Krakauer: First-principles study of piezoelectricity in tetragonal PbTiO_3 and $\text{PbZr}_{1/2}\text{Ti}_{1/2}\text{O}_3$, *Phys. Rev. B* **59**, 12771 (1999) [56](#)
- [41] L. Bellaiche, D. Vanderbilt: Intrinsic piezoelectric response in perovskite alloys: PMN-PT versus PZT, *Phys. Rev. Lett.* **83**, 1347 (1999) [56](#)
- [42] D. Vanderbilt: Berry-phase theory of proper piezoelectric response, *J. Phys. Chem. Solids* **61**, 147 (2000) [56](#), [57](#)
- [43] R. W. Nunes, D. Vanderbilt: Real-space approach to calculation of electric polarization and dielectric constants, *Phys. Rev. Lett.* **73**, 712 (1994) [58](#)
- [44] R. W. Nunes, X. Gonze: Berry-phase treatment of the homogeneous electric field perturbation in insulators, *Phys. Rev. B* **63**, 155107 (2001) [58](#)

- [45] I. Souza, J. Ñíguez, D. Vanderbilt: First-principles approach to insulators in finite electric fields, *Phys. Rev. Lett.* **89**, 117602 (2002) [58](#)
- [46] P. Umari, A. Pasquarello: Ab initio molecular dynamics in a finite homogeneous electric field, *Phys. Rev. Lett.* **89**, 157602 (2002) [58](#)
- [47] I. Souza, J. Ñíguez, D. Vanderbilt: Dynamics of Berry-phase polarization in time-dependent electric fields, *Phys. Rev. B* **69**, 085106 (2004) [58](#)
- [48] J. Ñíguez, L. Bellaiche, D. Vanderbilt: First-principles study of $(\text{BiScO}_3)_{1-x}-(\text{PbTiO}_3)_x$ piezoelectric alloys, *Phys. Rev. B* **67**, 224107 (2003) [60](#)
- [49] G. Ortiz, R. M. Martin: Macroscopic polarization as a geometric quantum phase: Many-body formulation, *Phys. Rev. B* **49**, 14 202 (1994) [61](#)
- [50] R. Resta: Quantum-mechanical position operator in extended systems, *Phys. Rev. Lett.* **80**, 1800 (1998) [61](#)
- [51] I. Souza, T. Wilkens, R. M. Martin: Polarization and localization in insulators: Generating function approach, *Phys. Rev. B* **62**, 1666 (2000) [61](#), [64](#)
- [52] R. Resta: Why are insulators insulating and metals conducting?, *J. Phys. Condens. Matter* **14**, R625 (2002) [61](#), [63](#)
- [53] X. Gonze, P. Ghosez, R. W. Godby: Density-polarization functional theory of the response of a periodic insulating solid to an electric field, *Phys. Rev. Lett.* **74**, 4035 (1995) [62](#)
- [54] X. Gonze, P. Ghosez, R. W. Godby: Density-functional theory of polar insulators, *Phys. Rev. Lett.* **78**, 294 (1997) [62](#)
- [55] D. Vanderbilt: Nonlocality of Kohn-Sham exchange-correlation fields in dielectrics, *Phys. Rev. Lett.* **79**, 3966 (1997) [62](#)
- [56] W. Kohn: Theory of the insulating state, *Phys. Rev.* **133**, A171 (1964) [63](#)
- [57] N. Marzari, D. Vanderbilt: Maximally localized generalized Wannier functions for composite energy bands, *Phys. Rev. B* **56**, 12847 (1997) [63](#), [64](#)
- [58] R. Resta, S. Sorella: Electron localization in the insulating state, *Phys. Rev. Lett.* **82**, 370 (1999) [63](#)

Index

- alloys, [56](#)
- BaTiO₃, [50](#), [55](#)
- Berry connection, [43](#)
- Berry phase, [31](#), [42](#), [43](#), [45](#), [61](#)
 finite-difference representation, [44](#)
- Bloch
 functions, [57](#), [58](#)
 orbitals, [63](#)
 states, [50](#), [51](#)
 theorem, [41](#), [57](#)
 wavefunctions, [31](#)
- boundary condition, [42](#)
- branch choice, [45–48](#), [50](#), [53](#), [59](#), [60](#)
- Brillouin zone, [31](#), [44–46](#)
- centers, [33](#)
 polarization, [33](#)
- centrosymmetric structure, [39](#)
- charge, [33](#)
 Born, [36](#), [54–56](#)
 dynamical, [36](#), [41](#), [54](#)
 electronic, [33](#)
 induced, [33](#)
 induced polarization, [33](#)
 interface, [59](#), [60](#)
 ionic, [49](#)
 periodic, [34](#)
 polarization, [41](#), [51](#)
 surface, [34](#), [59](#), [60](#)
 transport, [52](#)

- Clausius–Mossotti model, 32–34, 37
 CM, 51
 conductivity, 64
 current, 37, 43, 56
 adiabatic, 40, 47, 52
 macroscopic, 39
 transient, 37, 40
 density matrix, 58
 density-functional theory, 62
 Kohn–Sham, 42, 53, 62
 dielectric tensor, 33, 41
 disordered systems, 61
 domain wall, 59
 electric, 41
 electric field, 54, 57, 58, 62
 applied, 57
 exchange-correlation, 62
 finite, 57, 58
 force induced by, 54
 macroscopic, 57
 field
 depolarizing, 41
 global, 45
 Hohenberg–Kohn theorem, 62
 hysteresis cycle, 39
 hysteresis loop, 39
 insulator, 63
 ionic model, 49
 KNbO₃, 48–50, 53, 55
 lattice dynamics, 55
 localization, 63
 metals, 63
 PbTiO₃, 38, 56
 permittivity, 36, 37, 41
 perovskite, 38, 48, 53–55, 60
 perturbation theory, 42, 43
 phase, 40
 mod 2π , 46
 twist, 47
 piezoelectric tensor, 36, 41, 55
 proper, 56
 piezoelectricity, 36, 37, 41, 55
 polarization, 31
 absolute, 32
 Berry-phase, 41, 50, 51, 54, 58, 59, 62
 bulk, 34, 35
 change, 47, 56
 differences, 32, 38
 effective, 40, 43, 44, 50
 electronic, 33, 58, 61
 formal, 40, 44, 47–50
 induced, 40
 ionic, 44, 47
 local, 62
 longitudinal, 62
 macroscopic, 31, 32, 35, 37, 41, 54, 61, 63
 many-body, 61
 microscopic, 35
 modern theory, 35, 38, 41, 47, 54
 modern theory of, 31, 32, 43, 47, 53, 63
 multivalued, 50
 quantum, 46, 48, 50, 57
 quantum of, 31, 47, 51, 60
 reversal, 38, 39
 spontaneous, 35, 38–41, 43, 48, 50, 53, 56
 time-averaged, 53
 transverse, 62
 pyroelectric coefficient, 36
 silicon, 33, 34
 strain
 internal, 56
 macroscopic, 55, 56
 surface, 36, 55
 symmetry, 48, 50, 54
 cubic, 50
 temperature, 36
 twist operator, 61
 Wannier center, 50–52
 Wannier function, 50, 63, 64
 Zener tunneling, 57, 58